

# Synthesis, Gallium-68 Radiolabelling and Biological Analysis of a Series of Triarylphosphonium-Functionalized DO3A Chelators

## Supporting Information

Adam J. Smith,<sup>†,‡</sup> Peter J. Gawne,<sup>‡</sup> Michelle T. Ma,<sup>‡</sup> Philip J. Blower,<sup>‡</sup>  
Richard Southworth,<sup>\*,‡</sup> Nicholas J. Long<sup>\*,†</sup>

<sup>†</sup>*Department of Chemistry, Imperial College London, South Kensington, London, SW7 2AZ, U.K.*

<sup>‡</sup>*Division of Imaging Sciences and Biomedical Imaging, St. Thomas' Hospital, King's College London, London, SE1 7EH, U.K.*

## Contents

NMR Spectra .....	S3
Tri-p-tolylphosphane ( <b>1b</b> ).....	S3
(4-(Bromomethyl)benzyl)triphenylphosphonium bromide ( <b>2a</b> ).....	S4
(4-(Bromomethyl)benzyl)tri-p-tolylphosphonium bromide ( <b>2b</b> ).....	S6
(4-(Bromomethyl)benzyl)tris(3,5-dimethylphenyl)phosphonium bromide ( <b>2c</b> ).....	S7
Triphenyl(4-((4,7,10-tris(2-(tert-butoxy)-2-oxoethyl)-1,4,7,10-tetraazacyclododecan-1-yl)methyl)benzyl)phosphonium bromide ( <b>3a</b> ) .....	S9
Tri-p-tolyl(4-((4,7,10-tris(2-(tert-butoxy)-2-oxoethyl)-1,4,7,10-tetraazacyclododecan-1-yl)methyl)benzyl)phosphonium bromide ( <b>3b</b> ).....	S10
Tris(3,5-dimethylphenyl)(4-((4,7,10-tris(2-(tert-butoxy)-2-oxoethyl)-1,4,7,10-tetraazacyclododecan-1-yl)methyl)benzyl)phosphonium bromide ( <b>3c</b> ) .....	S12
DO3A-xy-TPP Trifluoroacetate.....	S14
DO3A-xy-TTP Trifluoroacetate .....	S16
DO3A-xy-TXP Trifluoroacetate .....	S18
iTLC Analysis.....	S20
RadioHPLC Analysis.....	S21
$[^{68}\text{Ga}]\text{Ga}$ -DO3A-xy-TPP .....	S22
$[^{68}\text{Ga}]\text{Ga}$ -DO3A-xy-TTP .....	S22
$[^{68}\text{Ga}]\text{Ga}$ -DO3A-xy-TXP.....	S23
Langendorff Isolated Perfused Heart Model.....	S24
Stability Study.....	S24
Effects of 600 nM CCCP Infusion on Haemodynamic Parameters .....	S25
Triple $\gamma$ -Detector System Raw Data for MIBI Using the Two-Injection Protocol .....	S26
Triple $\gamma$ -Detector System Raw Data for $[^{68}\text{Ga}]\text{Ga}$ -DO3A-xy-TXP Using the Two-Injection Protocol .....	S28

## NMR Spectra

### Tri-*p*-tolylphosphane (**1b**)

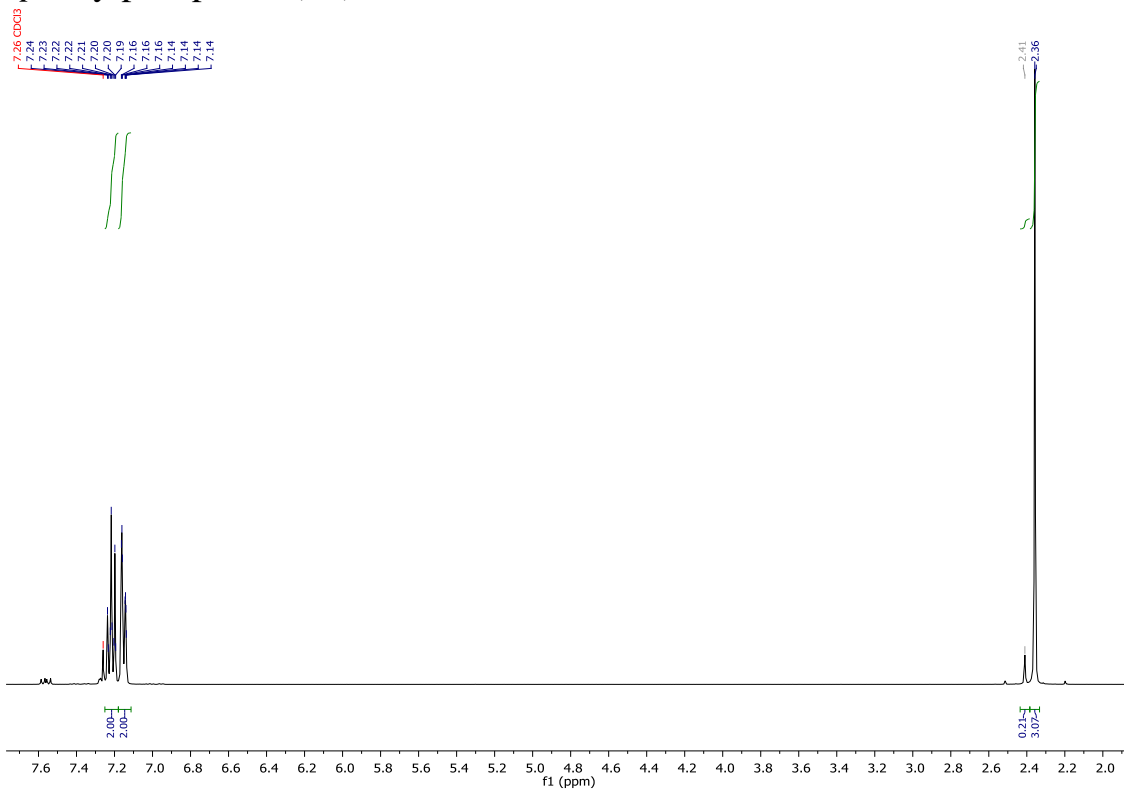


Figure S1:  $^1\text{H}$  NMR spectrum ( $\text{CDCl}_3$ , 400 MHz, 298 K)

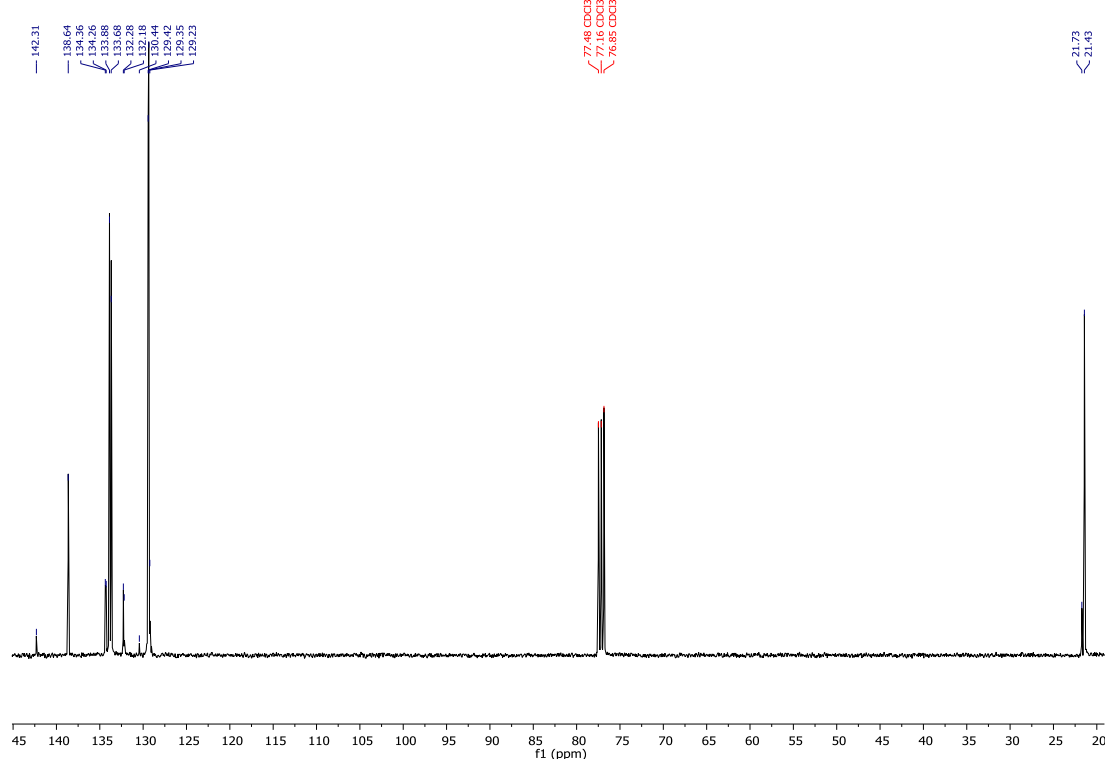


Figure S2:  $^{13}\text{C}\{\text{H}\}$  NMR spectrum ( $\text{CDCl}_3$ , 100 MHz, 298 K)

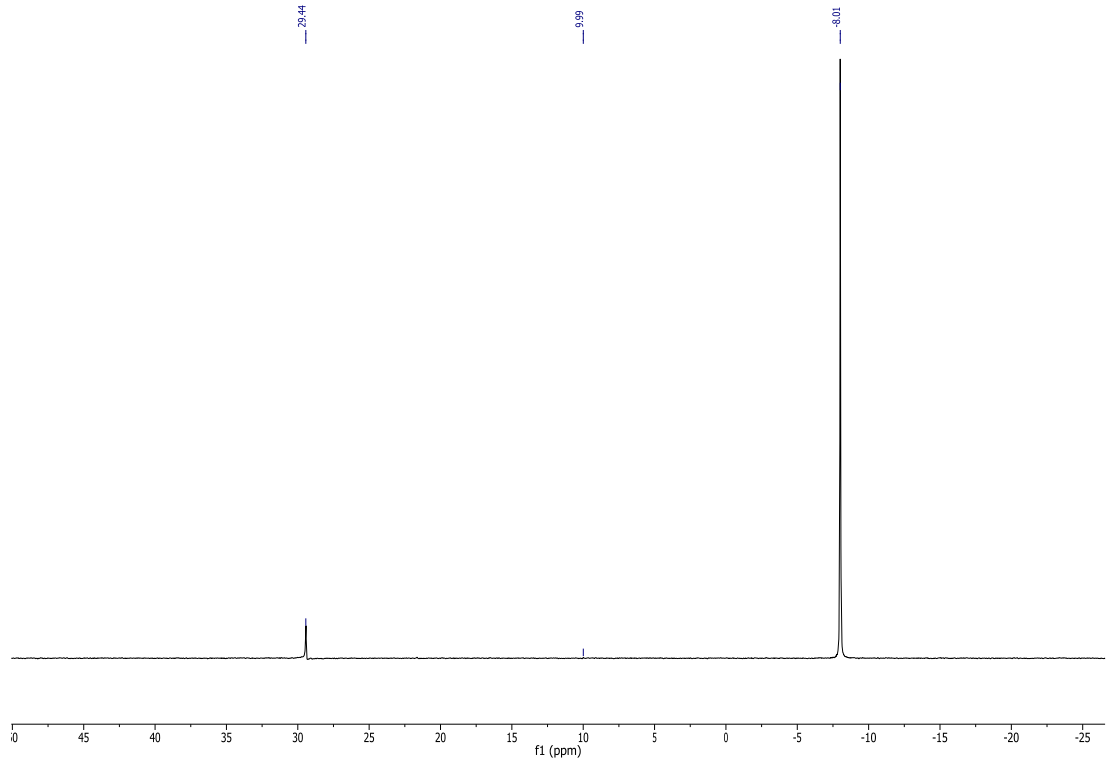


Figure S3:  $^{31}\text{P}\{\text{H}\}$  NMR spectrum ( $\text{CDCl}_3$ , 162 MHz, 298 K)

### (4-(Bromomethyl)benzyl)triphenylphosphonium bromide (**2a**)

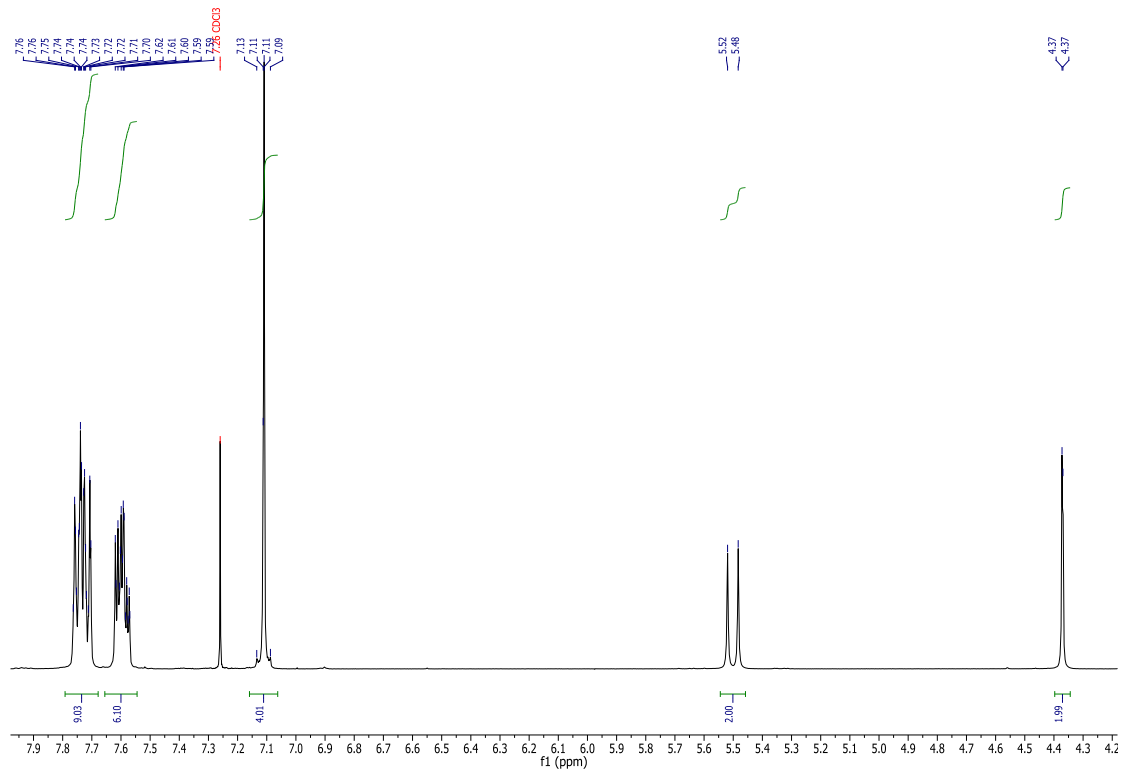


Figure S4:  $^1\text{H}$  NMR spectrum ( $\text{CDCl}_3$ , 400 MHz, 298 K)

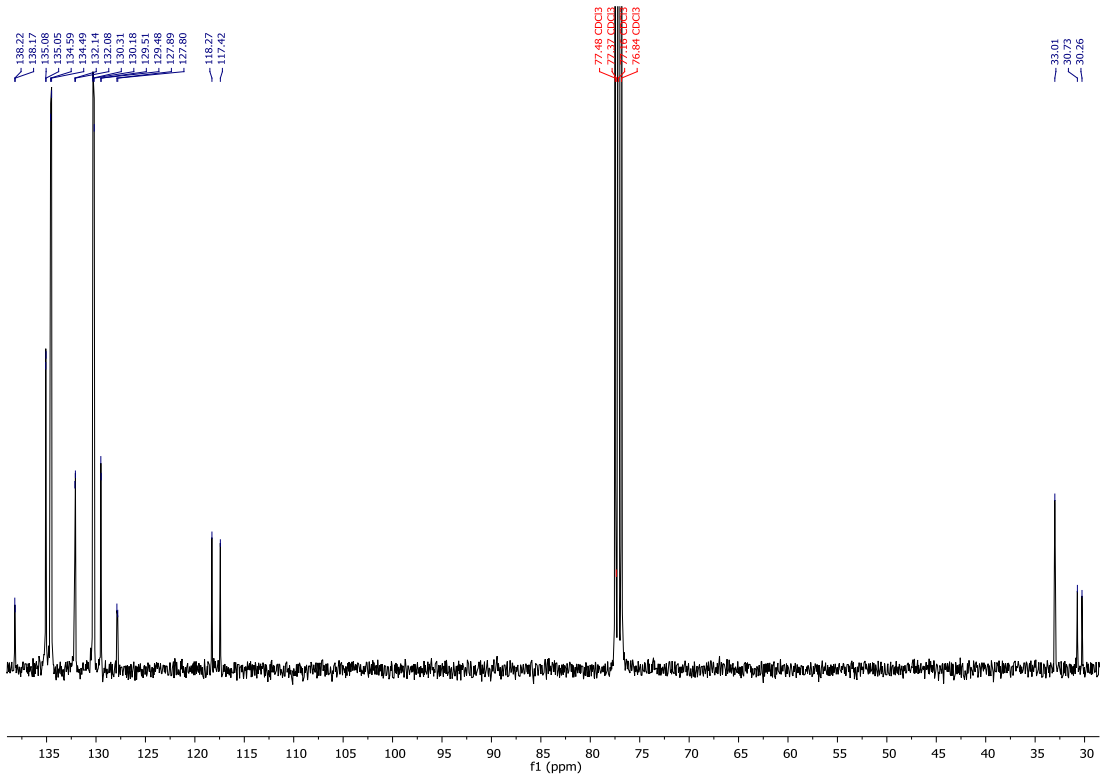


Figure S5:  $^{13}\text{C}\{\text{H}\}$  NMR spectrum ( $\text{CDCl}_3$ , 100 MHz, 298 K). The residual solvent peak has been truncated for clarity.

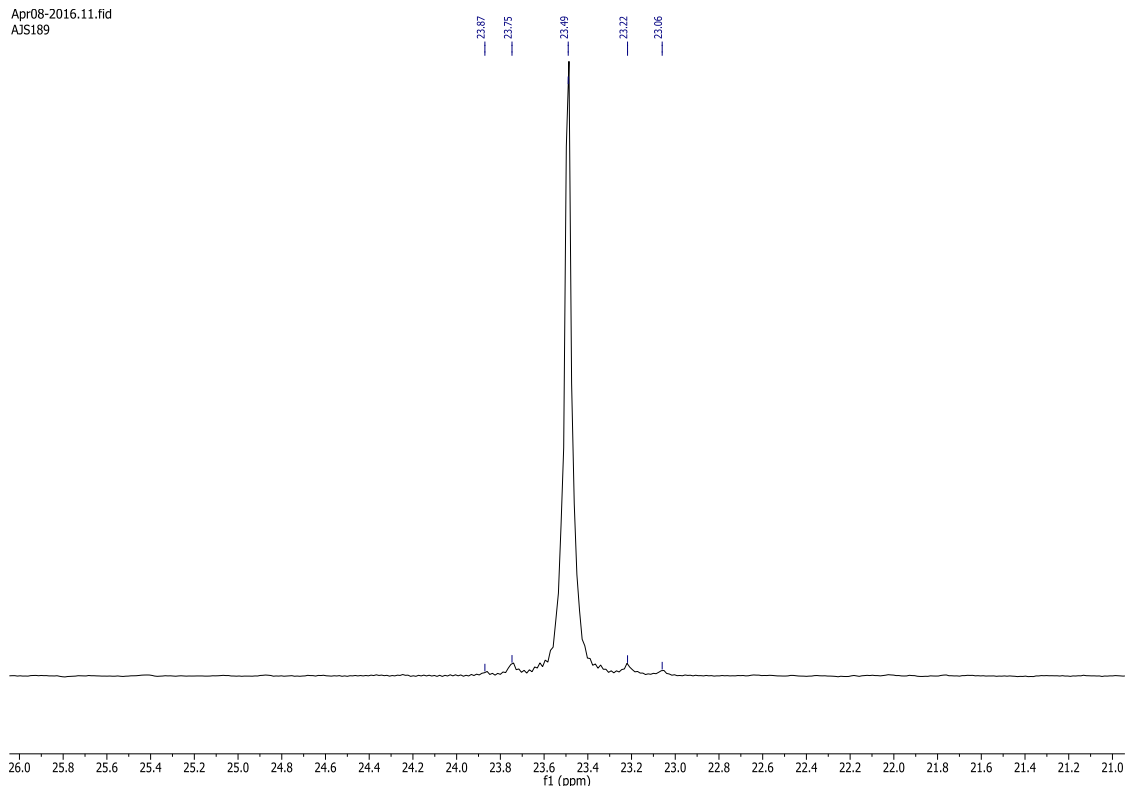


Figure S6:  $^{31}\text{P}\{\text{H}\}$  NMR spectrum ( $\text{CDCl}_3$ , 162 MHz, 298 K)

(4-(Bromomethyl)benzyl)tri-*p*-tolylphosphonium bromide (**2b**)

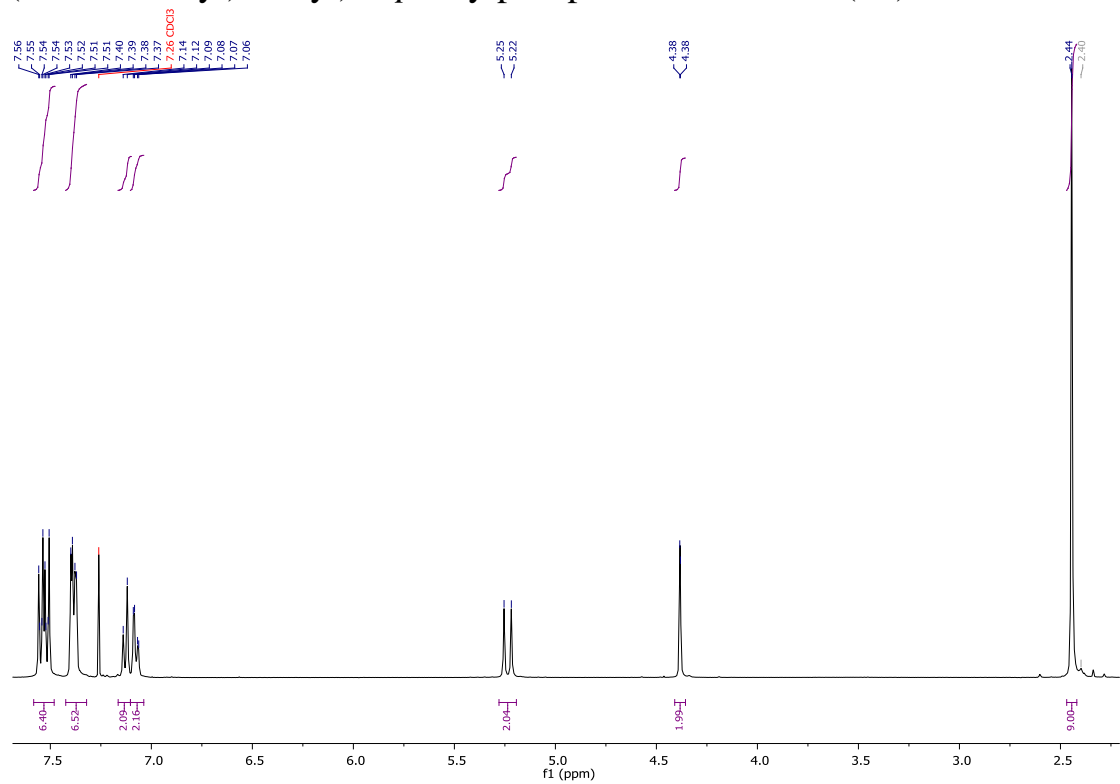


Figure S7:  $^1\text{H}$  NMR spectrum ( $\text{CDCl}_3$ , 400 MHz, 298 K)

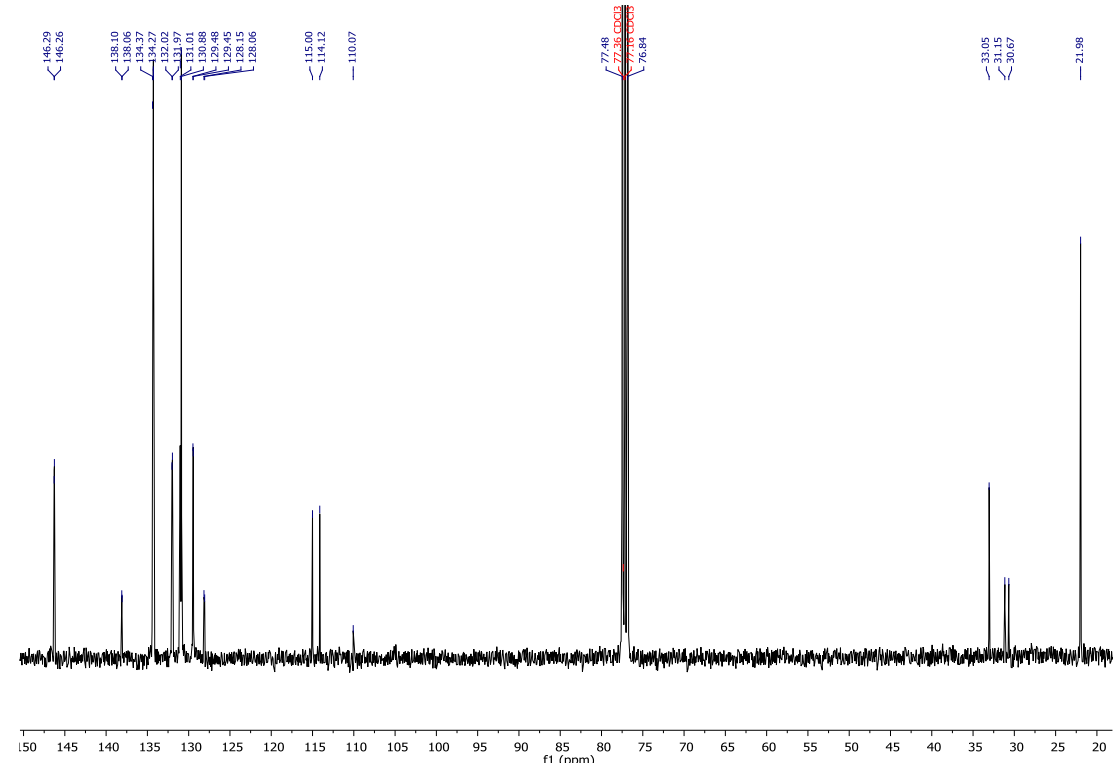


Figure S8:  $^{13}\text{C}\{^1\text{H}\}$  NMR spectrum ( $\text{CDCl}_3$ , 100 MHz, 298 K). The residual solvent peak has been truncated for clarity.

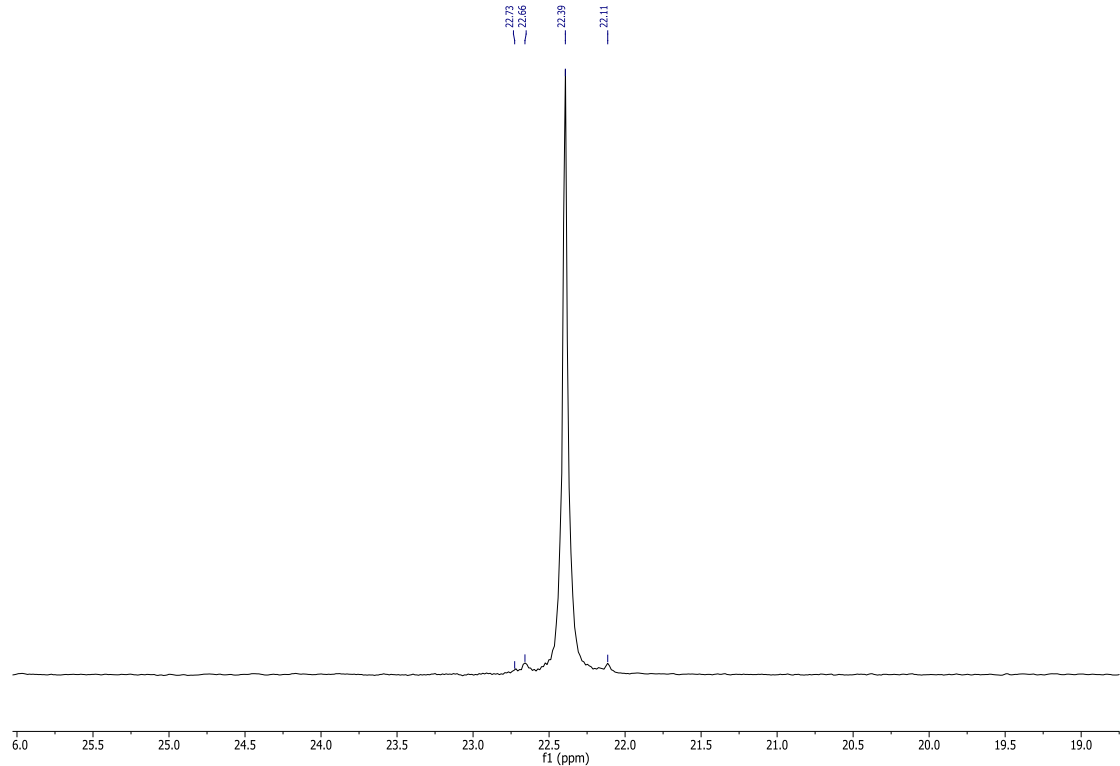


Figure S9:  $^{31}\text{P}\{\text{H}\}$  NMR spectrum ( $\text{CDCl}_3$ , 162 MHz, 298 K)

**(4-(Bromomethyl)benzyl)tris(3,5-dimethylphenyl)phosphonium bromide (**2c**)**

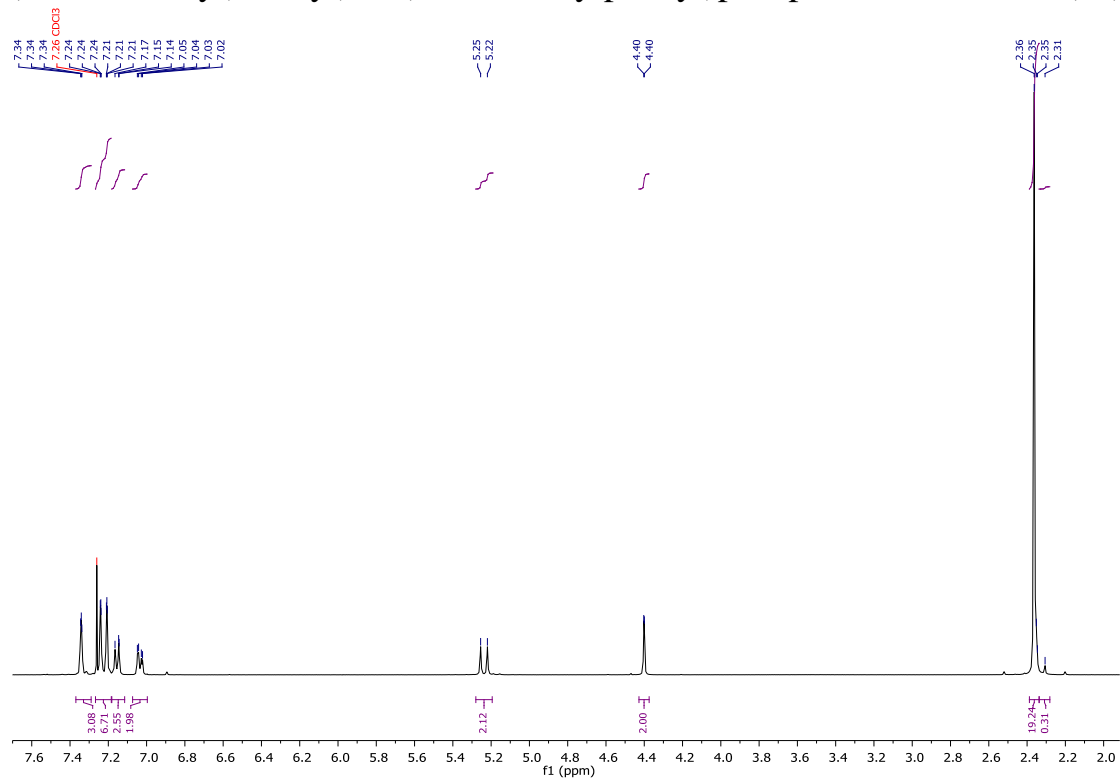


Figure S9:  $^1\text{H}$  NMR spectrum ( $\text{CDCl}_3$ , 400 MHz, 298 K)

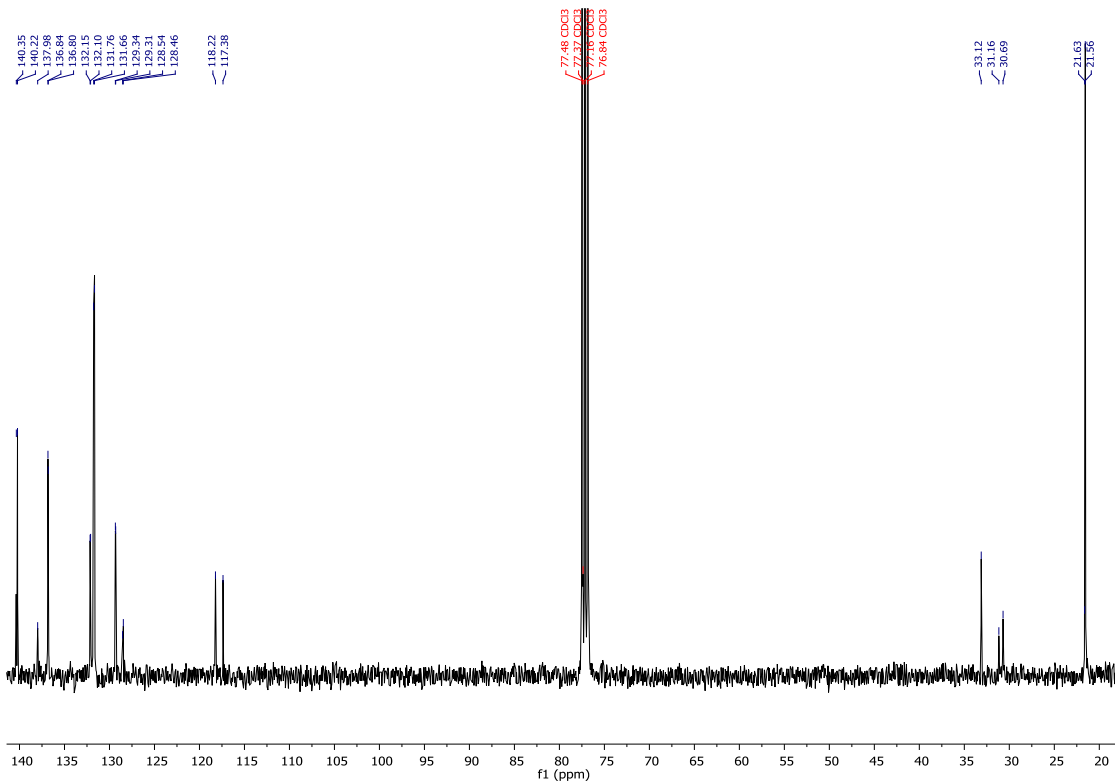


Figure S10:  $^{13}\text{C}\{^1\text{H}\}$  NMR spectrum ( $\text{CDCl}_3$ , 100 MHz, 298 K). The residual solvent peak has been truncated for clarity.

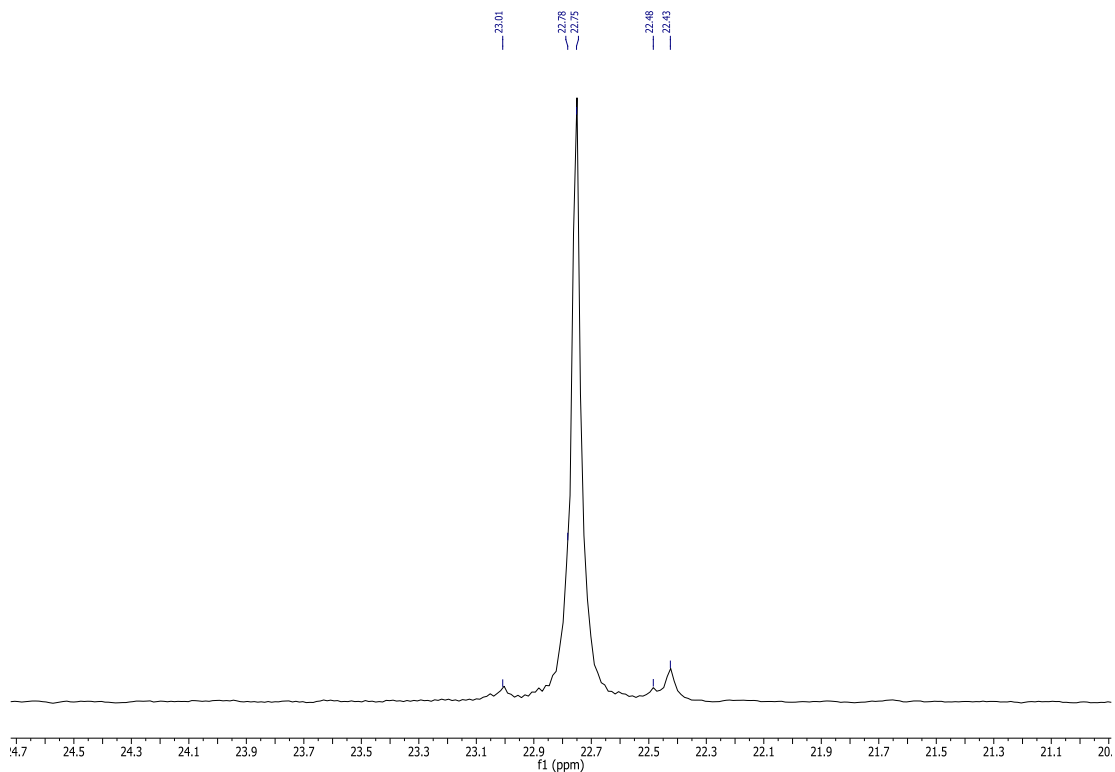


Figure S11:  $^{31}\text{P}\{^1\text{H}\}$  NMR spectrum ( $\text{CDCl}_3$ , 162 MHz, 298 K)

**Triphenyl(4-((4,7,10-tris(2-(*tert*-butoxy)-2-oxoethyl)-1,4,7,10-tetraazacyclododecan-1-yl)methyl)benzyl)phosphonium bromide (**3a**)**

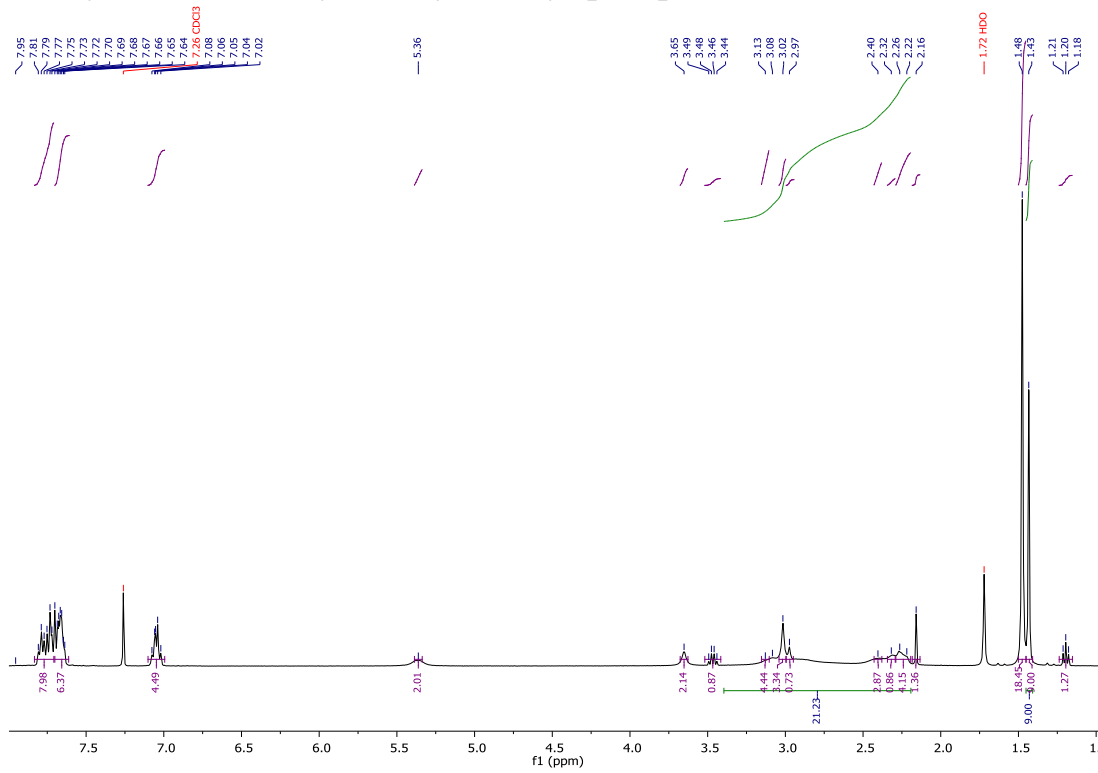


Figure S12:  $^1\text{H}$  NMR spectrum ( $\text{CDCl}_3$ , 400 MHz, 298 K)

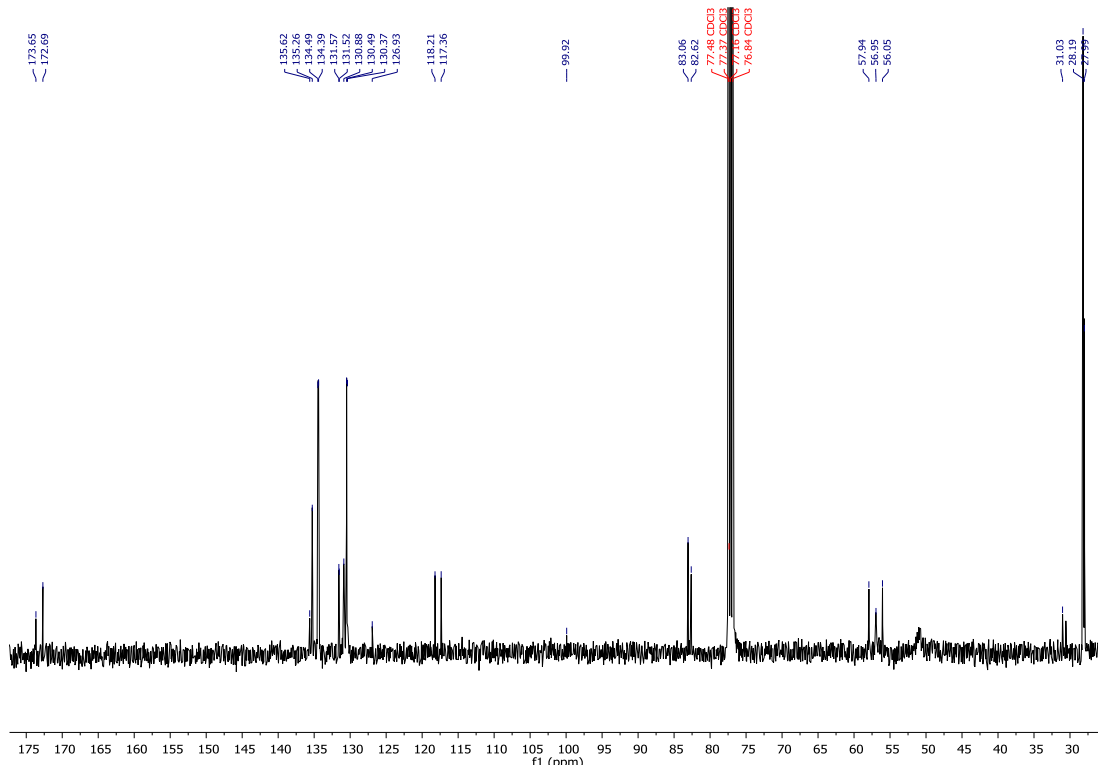


Figure S13:  $^{13}\text{C}\{\text{H}\}$  NMR spectrum ( $\text{CDCl}_3$ , 100 MHz, 298 K). The residual solvent peak has been truncated for clarity.

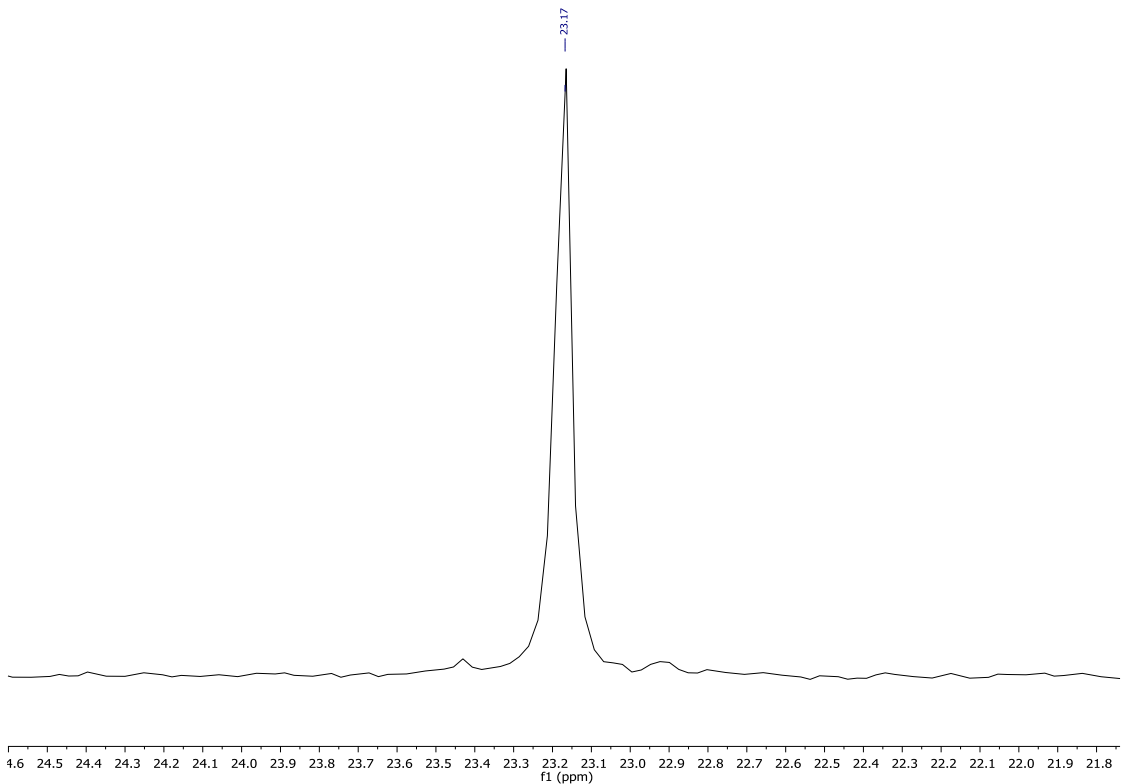


Figure S14:  $^{31}\text{P}\{\text{H}\}$  NMR spectrum ( $\text{CDCl}_3$ , 162 MHz, 298 K)

Tri-*p*-tolyl(4-((4,7,10-tris(2-(*tert*-butoxy)-2-oxoethyl)-1,4,7,10-tetraazacyclododecan-1-yl)methyl)benzyl)phosphonium bromide (**3b**)

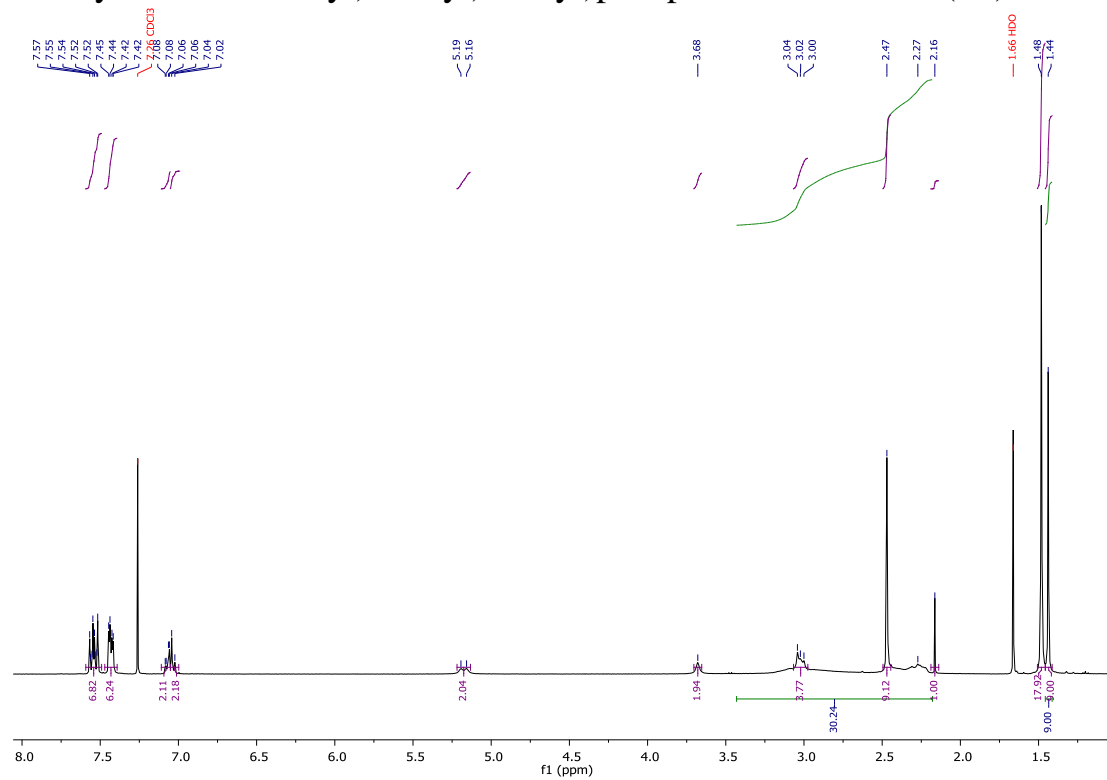


Figure S15:  $^1\text{H}$  NMR spectrum ( $\text{CDCl}_3$ , 400 MHz, 298 K)

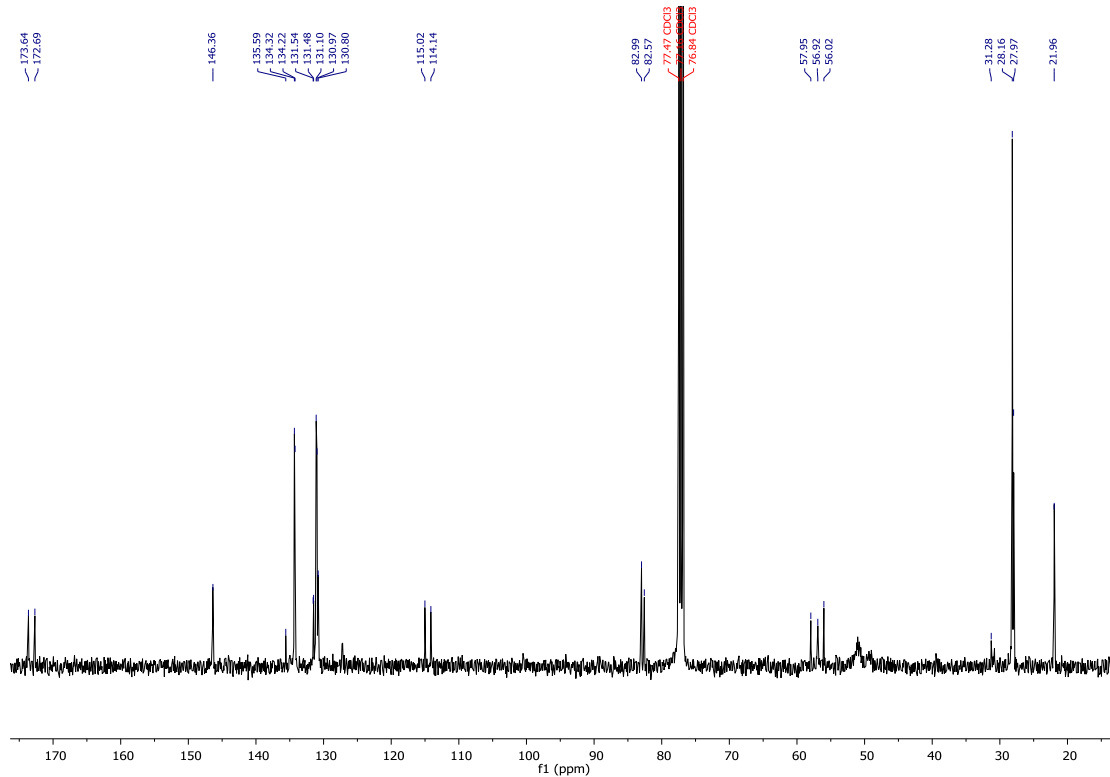


Figure S16:  $^{13}\text{C}\{^1\text{H}\}$  NMR spectrum ( $\text{CDCl}_3$ , 100 MHz, 298 K). The residual solvent peak has been truncated for clarity.

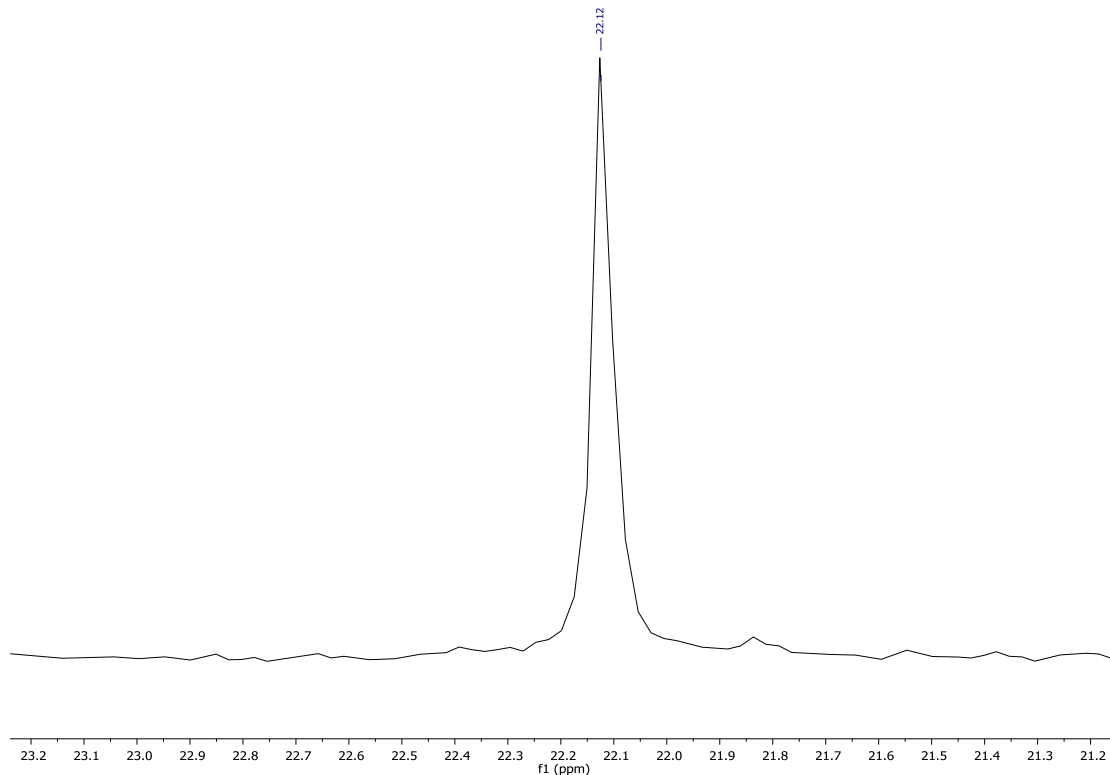


Figure S17:  $^{31}\text{P}\{^1\text{H}\}$  NMR spectrum ( $\text{CDCl}_3$ , 162 MHz, 298 K)

Tris(3,5-dimethylphenyl)(4-((4,7,10-tris(2-(*tert*-butoxy)-2-oxoethyl)-1,4,7,10-tetraazacyclododecan-1-yl)methyl)benzyl)phosphonium bromide (**3c**)

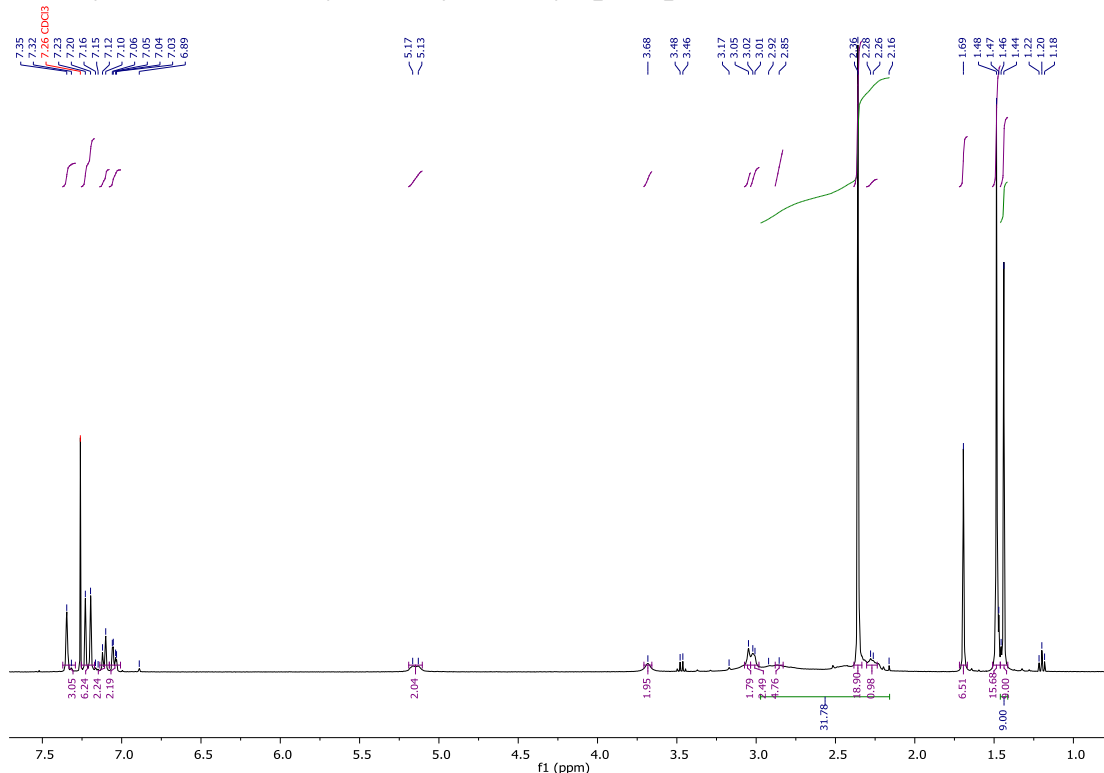


Figure S18:  $^1\text{H}$  NMR spectrum ( $\text{CDCl}_3$ , 400 MHz, 298 K)

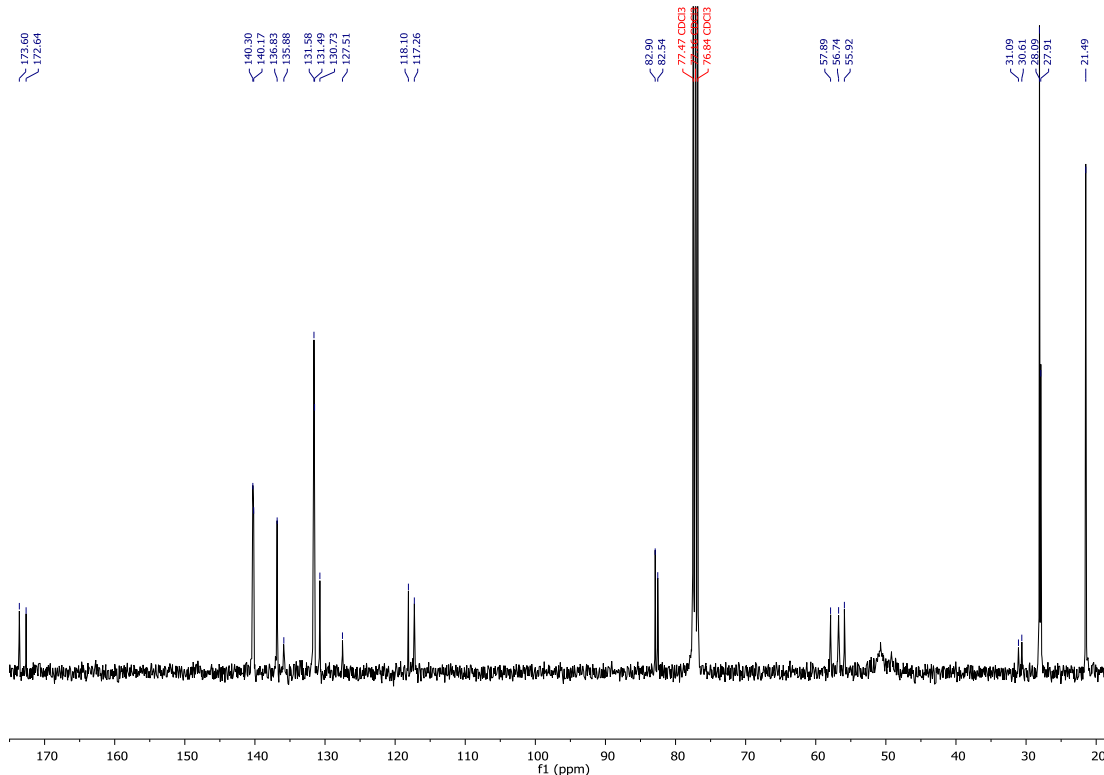


Figure S19:  $^{13}\text{C}\{^1\text{H}\}$  NMR spectrum ( $\text{CDCl}_3$ , 100 MHz, 298 K). The residual solvent peak has been truncated for clarity.

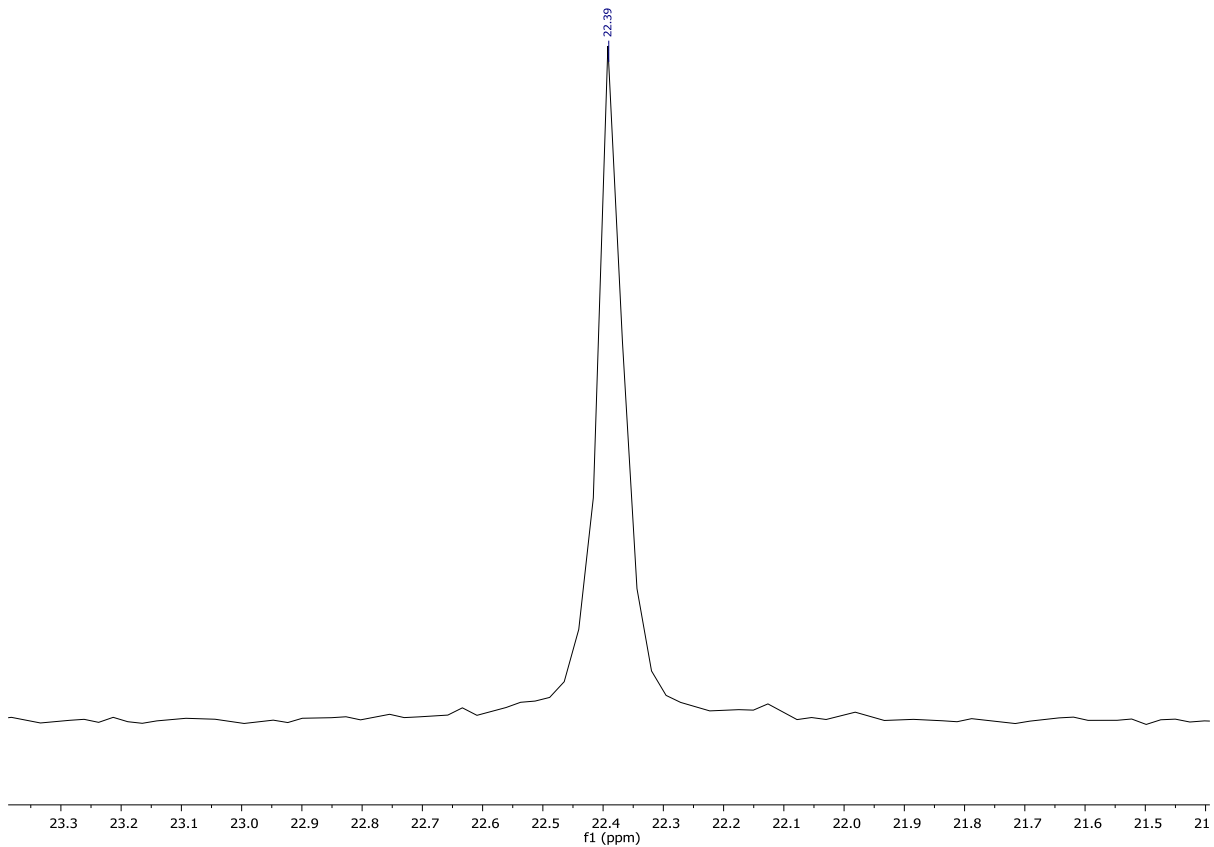


Figure S20:  $^{31}\text{P}\{\text{H}\}$  NMR spectrum ( $\text{CDCl}_3$ , 162 MHz, 298 K)

## DO3A-xy-TPP Trifluoroacetate

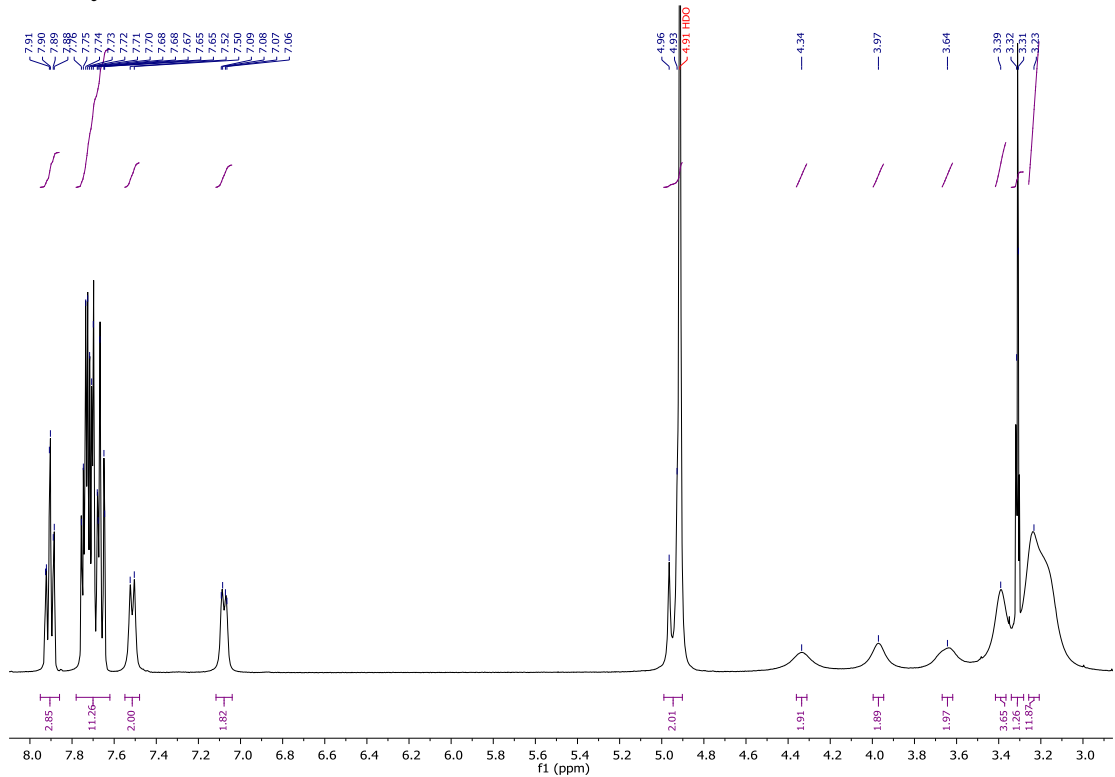


Figure S21:  $^1\text{H}$  NMR spectrum (MeOD, 400 MHz, 298 K). The residual solvent peak has been truncated for clarity.

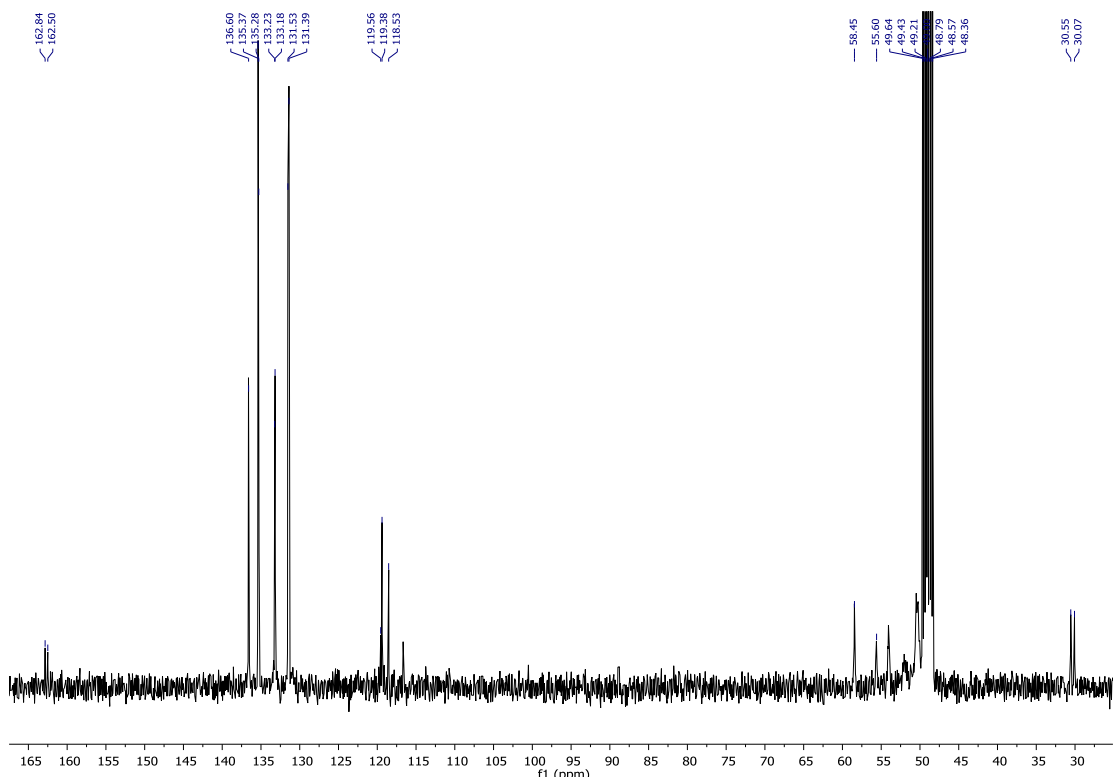


Figure S22:  $^{13}\text{C}\{^1\text{H}\}$  NMR spectrum (MeOD, 100 MHz, 298 K). The residual solvent peak has been truncated for clarity.

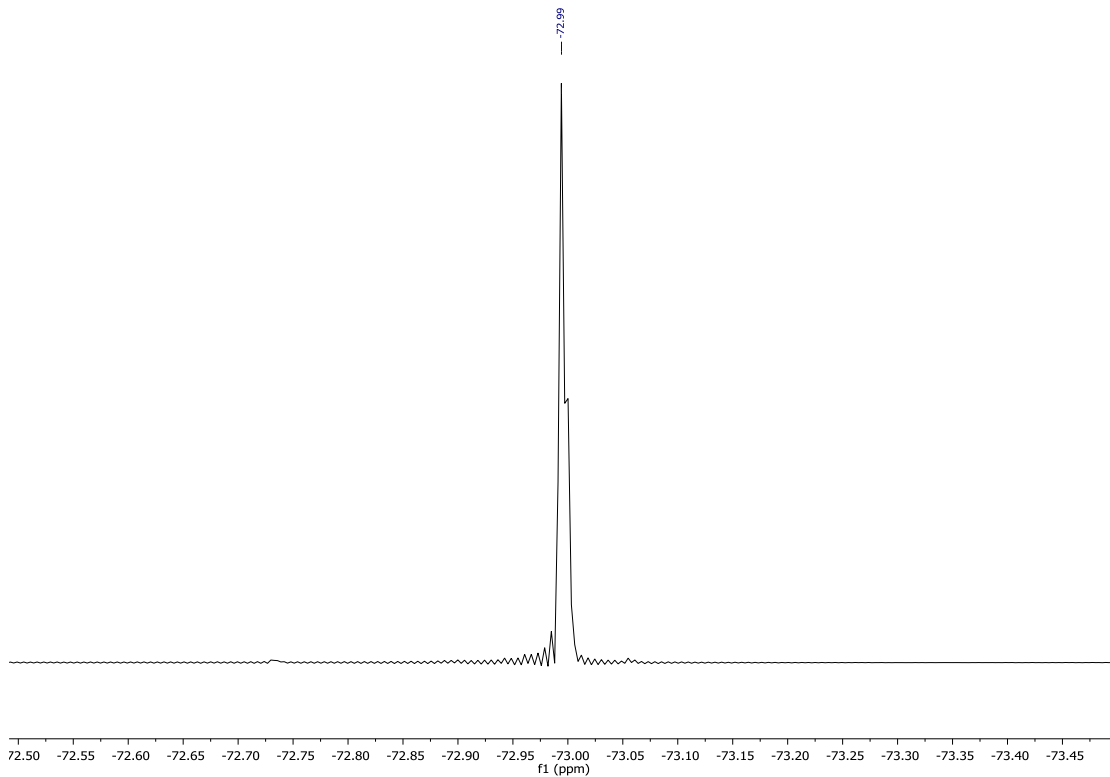


Figure S23:  $^{19}\text{F}\{\text{H}\}$  NMR spectrum (MeOD, 377 MHz, 298 K)

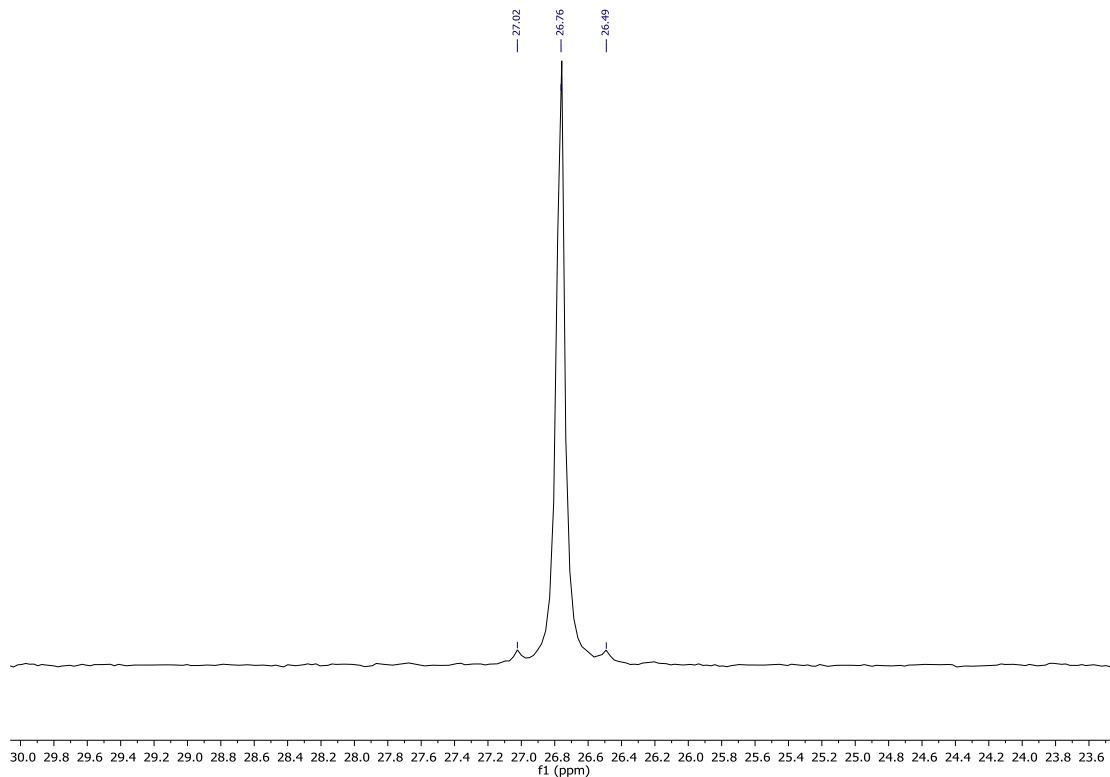


Figure S24:  $^{31}\text{P}\{\text{H}\}$  NMR spectrum (MeOD, 162 MHz, 298 K)

## DO3A-xy-TTP Trifluoroacetate

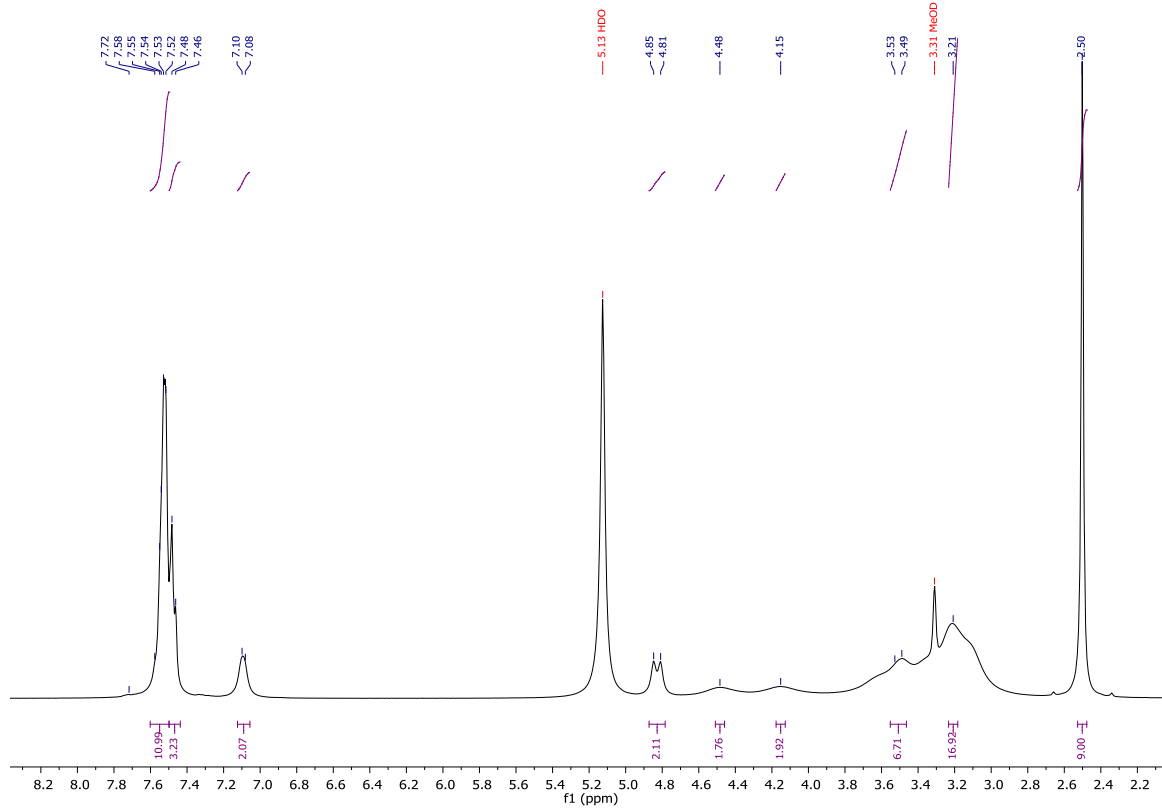


Figure S25:  $^1\text{H}$  NMR spectrum (MeOD, 400 MHz, 298 K).

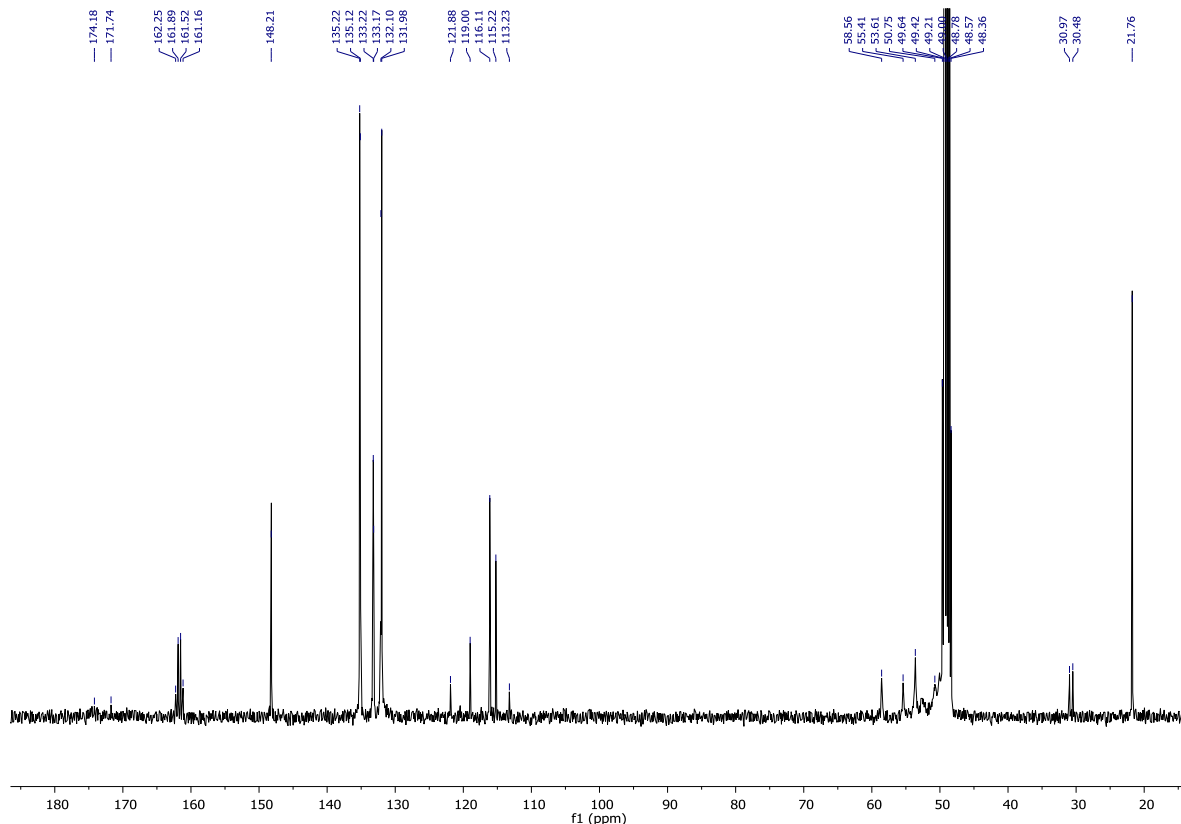


Figure S26:  $^{13}\text{C}\{\text{H}\}$  NMR spectrum (MeOD, 100 MHz, 298 K). The residual solvent peak has been truncated for clarity.

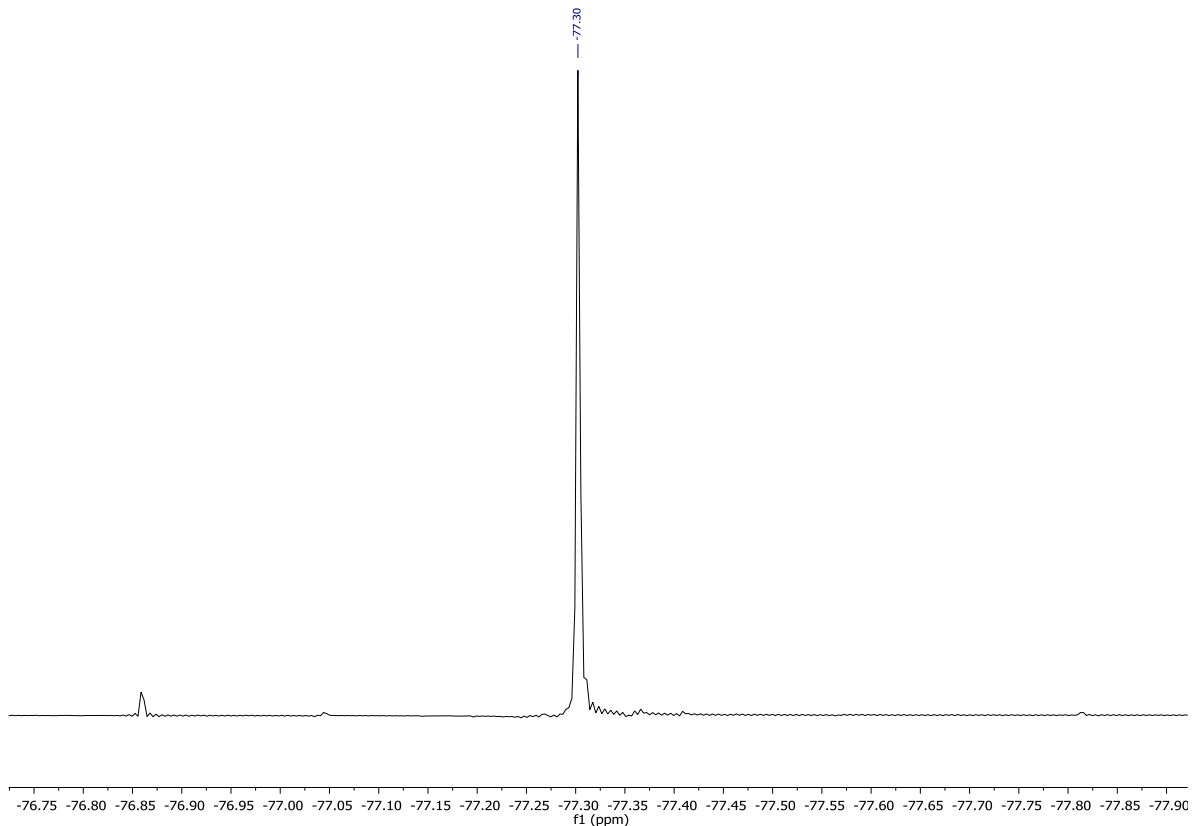


Figure S27:  $^{19}\text{F}\{\text{H}\}$  NMR spectrum (MeOD, 377 MHz, 298 K)

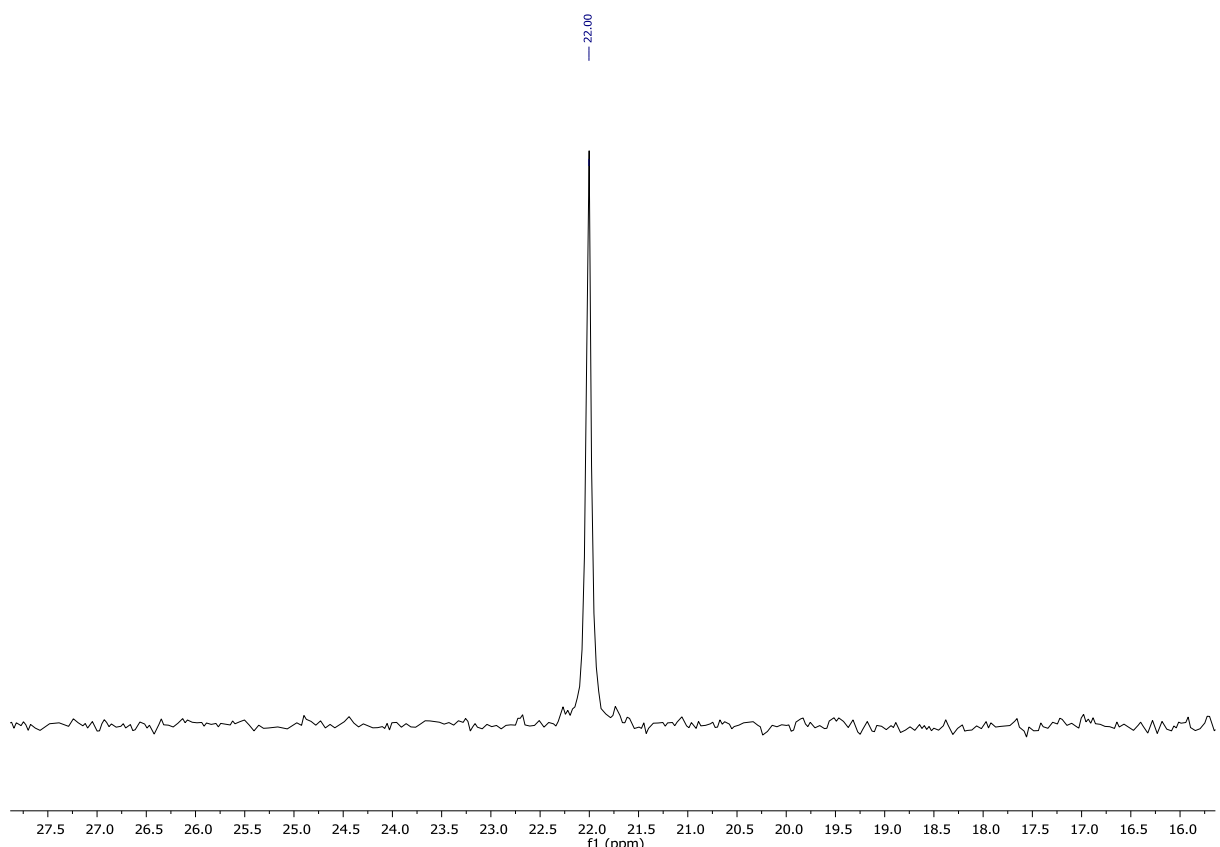


Figure S28:  $^{31}\text{P}\{\text{H}\}$  NMR spectrum (MeOD, 162 MHz, 298 K)

## DO3A-xy-TXP Trifluoroacetate

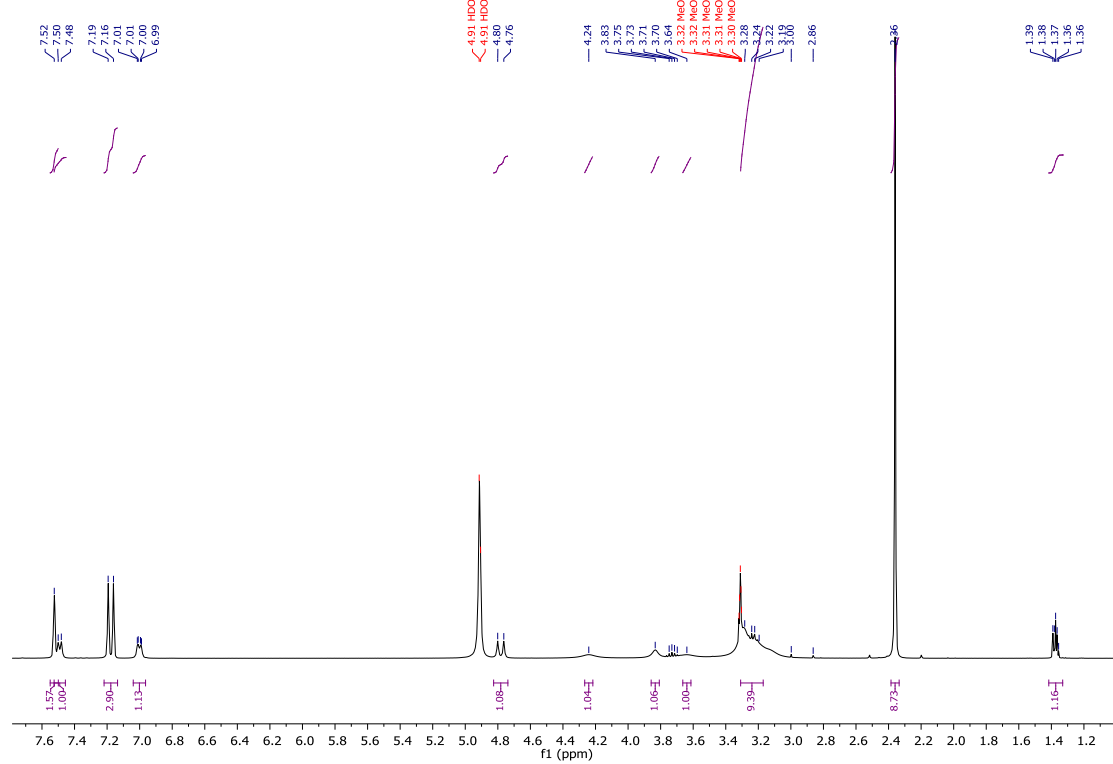


Figure S29:  $^1\text{H}$  NMR spectrum (MeOD, 400 MHz, 298 K)

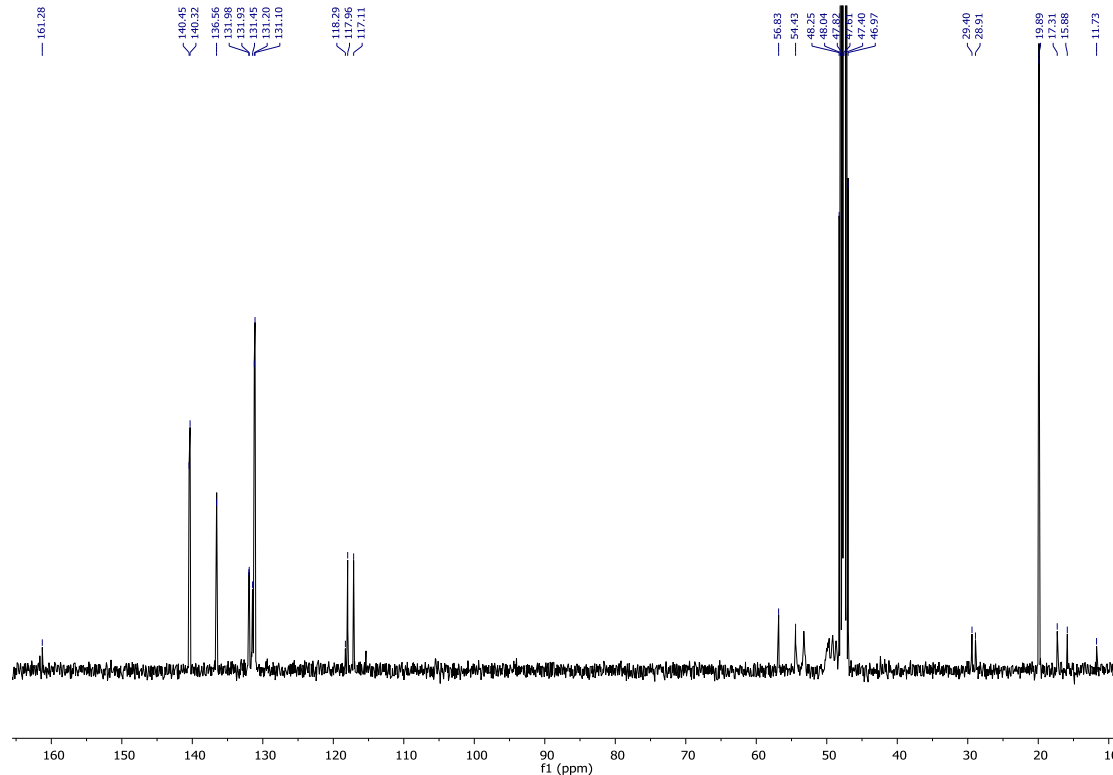


Figure S30:  $^{13}\text{C}\{\text{H}\}$  NMR spectrum (MeOD, 100 MHz, 298 K). The residual solvent peak has been truncated for clarity.

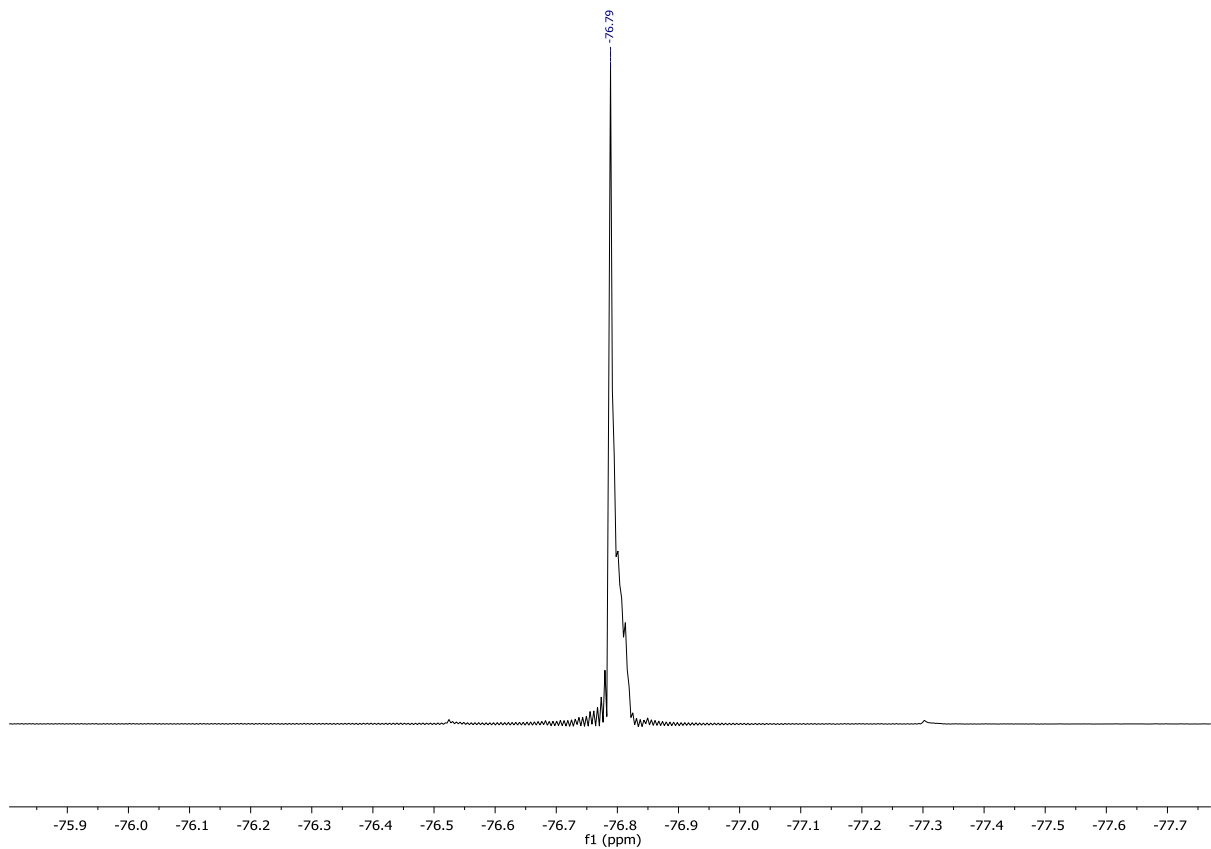


Figure S31:  $^{19}\text{F}\{\text{H}\}$  NMR spectrum (MeOD, 377 MHz, 298 K)

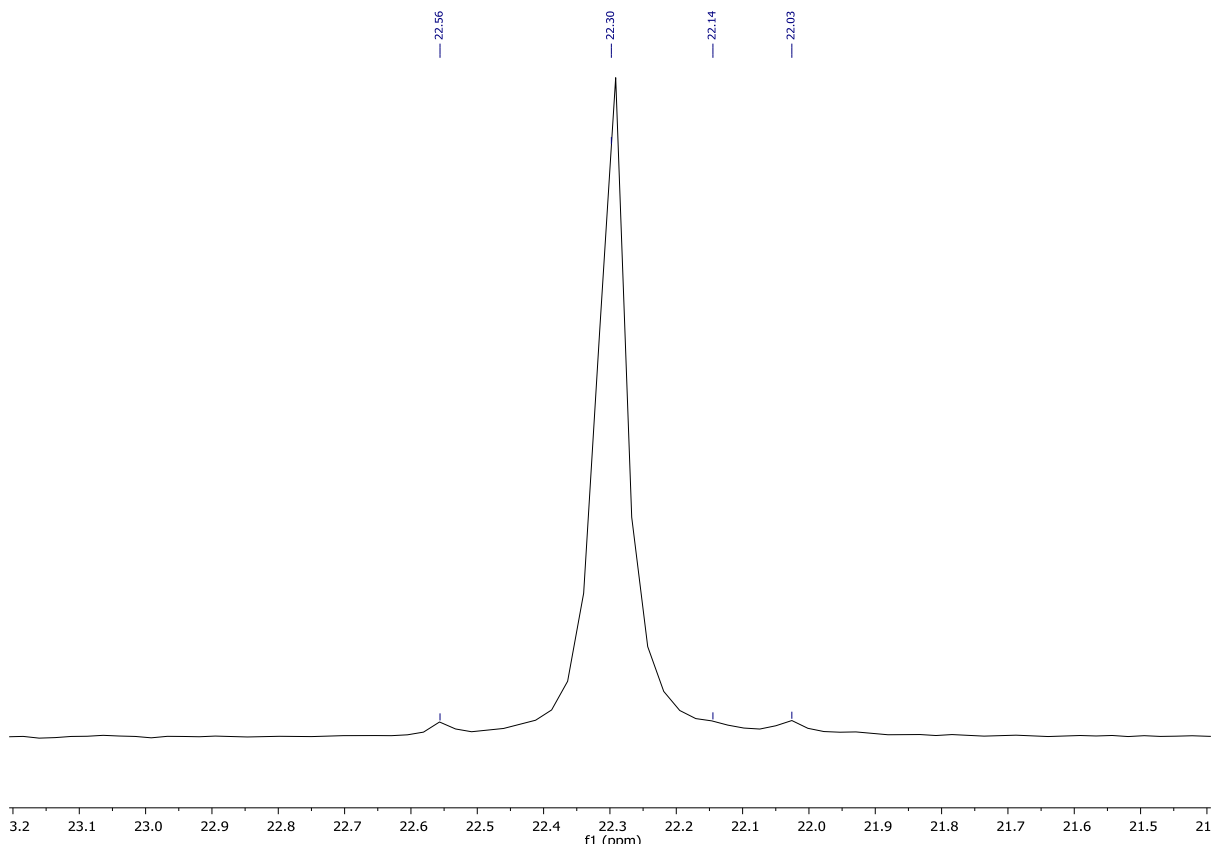


Figure S32:  $^{31}\text{P}\{\text{H}\}$  NMR spectrum (MeOD, 162 MHz, 298 K)

## iTLC Analysis

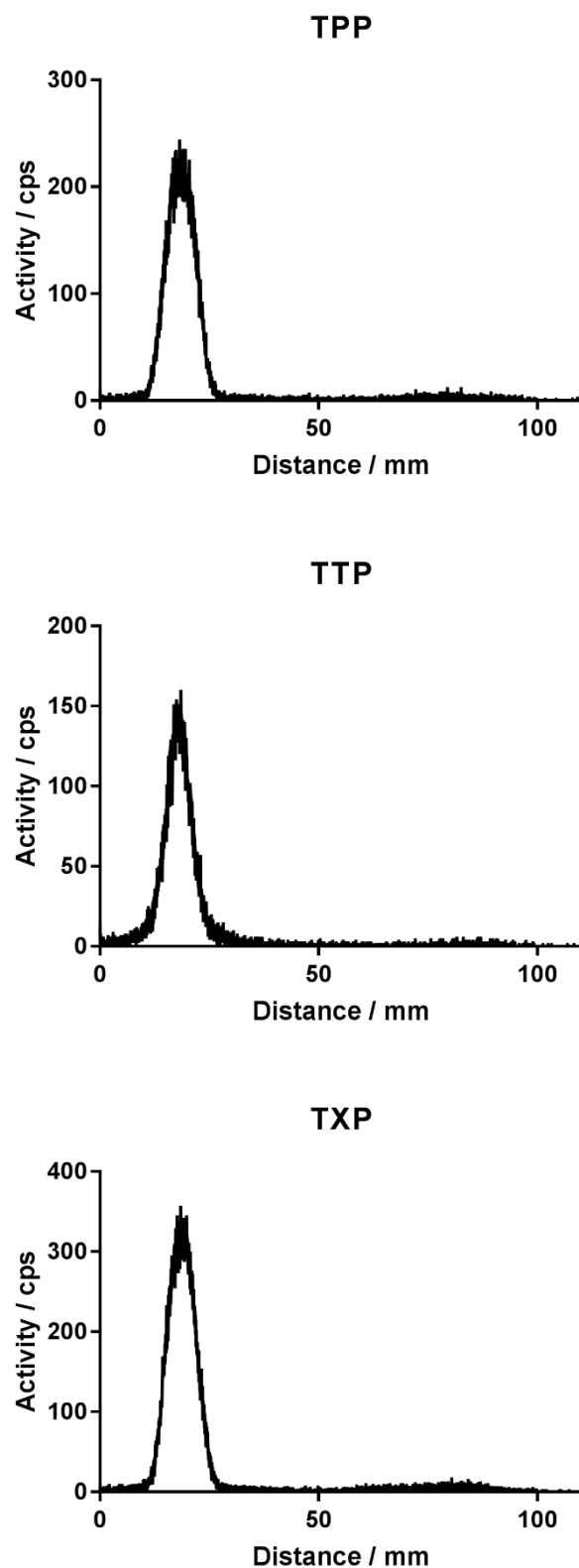


Figure S33: iTLC traces of  $[^{68}\text{Ga}]\text{Ga-DO3A-xy-TPP}$ ,  $[^{68}\text{Ga}]\text{Ga-DO3A-xy-TTP}$  and  $[^{68}\text{Ga}]\text{Ga-DO3A-xy-TXP}$ . Mobile phase: 0.1 M disodium EDTA.

RadioHPLC Analysis  
DO3A-xy-TAP

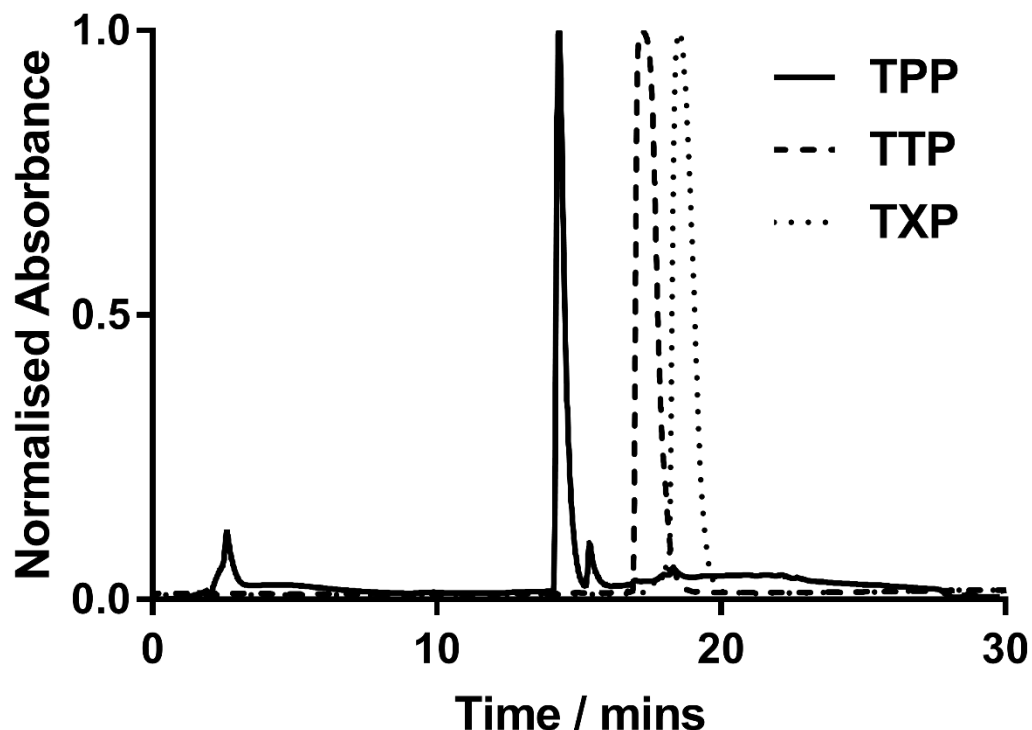


Figure S34: HPLC traces of DO3A-xy-TPP (solid), DO3A-xy-TTP (dashed) and DO3A-xy-TXP (dotted). Eluent gradient water (0.1 % TFA) (A) and MeCN (0.1 % TFA) (B) (isocratic 100 % A for 5 min; gradient 0 – 80 % B in A for 20 min, isocratic 100 % A for 5 min at a flow rate of 1 mL min<sup>-1</sup>). UV absorption  $\lambda_{\text{abs}} = 250$  nm.

[<sup>68</sup>Ga]Ga-DO3A-xy-TPP

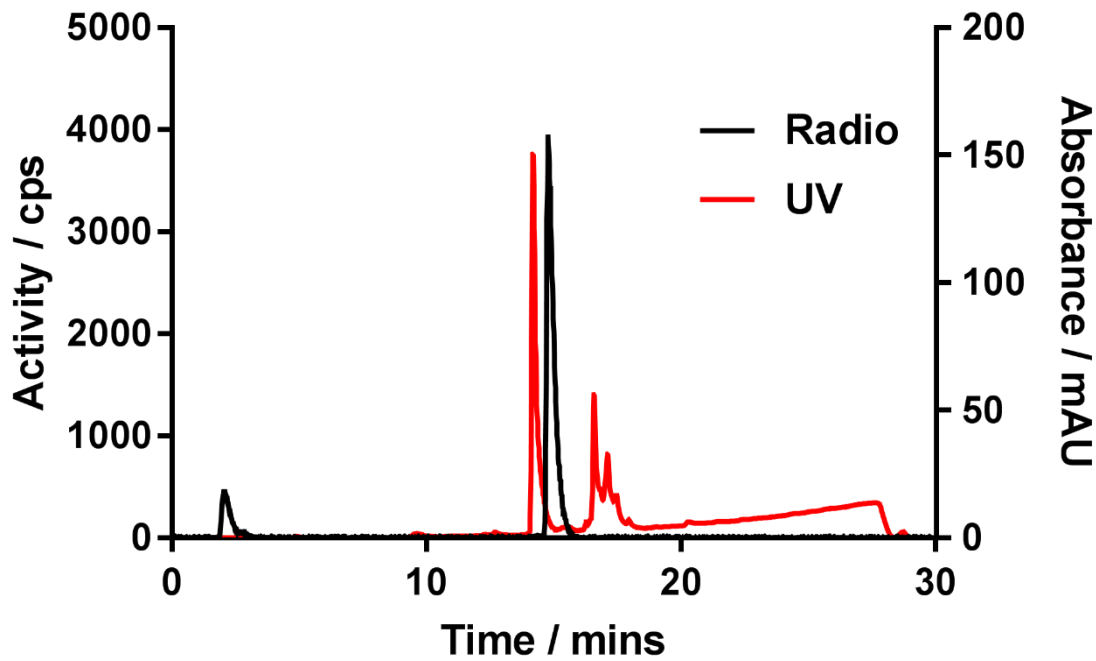


Figure S35: RadioHPLC trace of [<sup>68</sup>Ga]Ga-DO3A-xy-TPP. Eluent gradient: water (0.1 % TFA) (A) and MeCN (0.1 % TFA) (B) (isocratic 100 % A for 5 min; gradient 0 – 80 % B in A for 20 min, isocratic 100 % A for 5 min at a flow rate of  $1 \text{ mL min}^{-1}$ ). Radioactivity shown in black, UV absorption ( $\lambda_{\text{abs}} = 250 \text{ nm}$ ) shown in red.

[<sup>68</sup>Ga]Ga-DO3A-xy-TTP

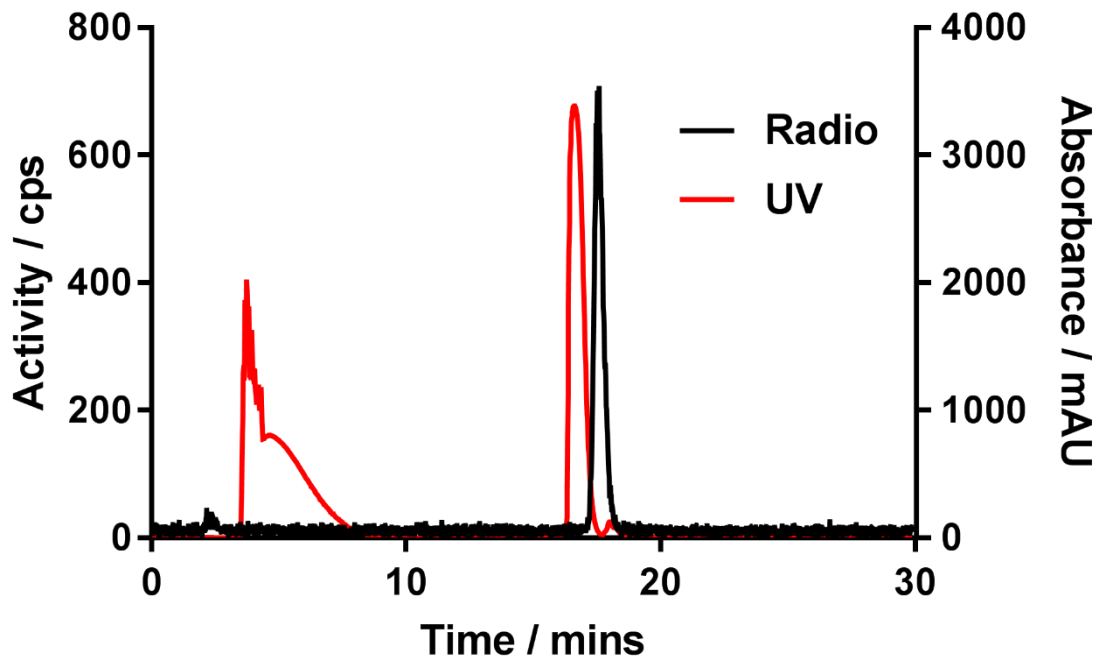


Figure S36: RadioHPLC trace of  $[^{68}\text{Ga}]\text{Ga-DO3A-xy-TTP}$ . Eluent gradient: water (0.1 % TFA) (A) and MeCN (0.1 % TFA) (B) (isocratic 100 % A for 5 min; gradient 0 – 80 % B in A for 20 min, isocratic 100 % A for 5 min at a flow rate of  $1 \text{ mL min}^{-1}$ ). Radioactivity shown in black, UV absorption ( $\lambda_{\text{abs}} = 250 \text{ nm}$ ) shown in red.

$[^{68}\text{Ga}]\text{Ga-DO3A-xy-TXP}$

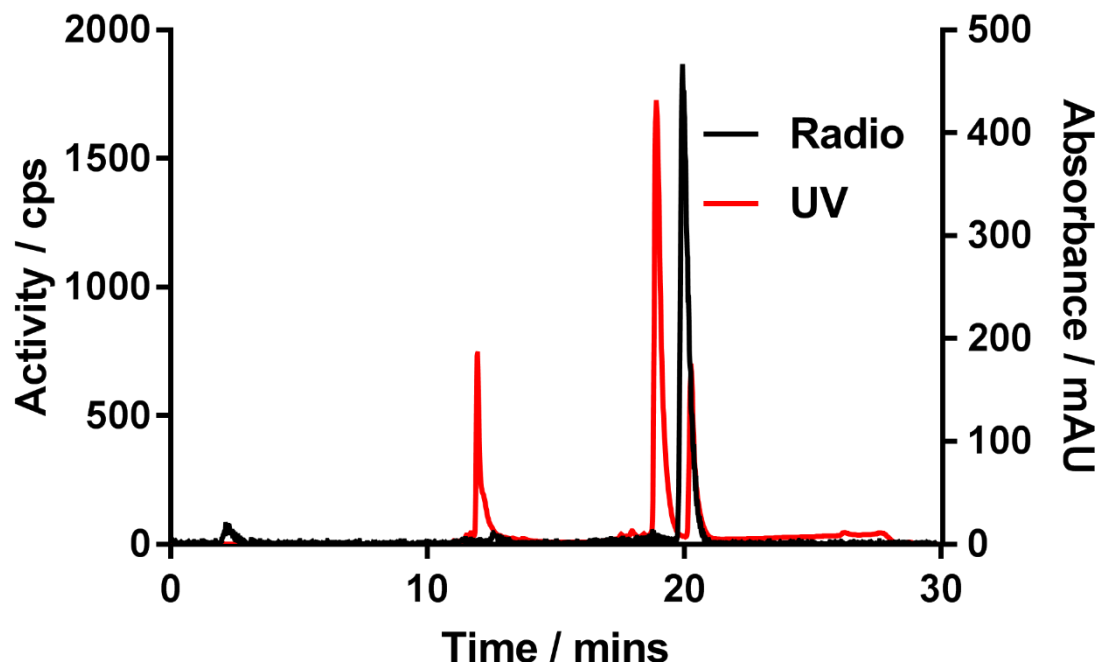


Figure S37: RadioHPLC trace of  $[^{68}\text{Ga}]\text{Ga-DO3A-xy-TXP}$ . Eluent gradient: water (0.1 % TFA) (A) and MeCN (0.1 % TFA) (B) (isocratic 100 % A for 5 min; gradient 0 – 80 % B in A for 20 min, isocratic 100 % A for 5 min at a flow rate of  $1 \text{ mL min}^{-1}$ ). Radioactivity shown in black, UV absorption ( $\lambda_{\text{abs}} = 250 \text{ nm}$ ) shown in red.

# Langendorff Isolated Perfused Heart Model

## Stability Study

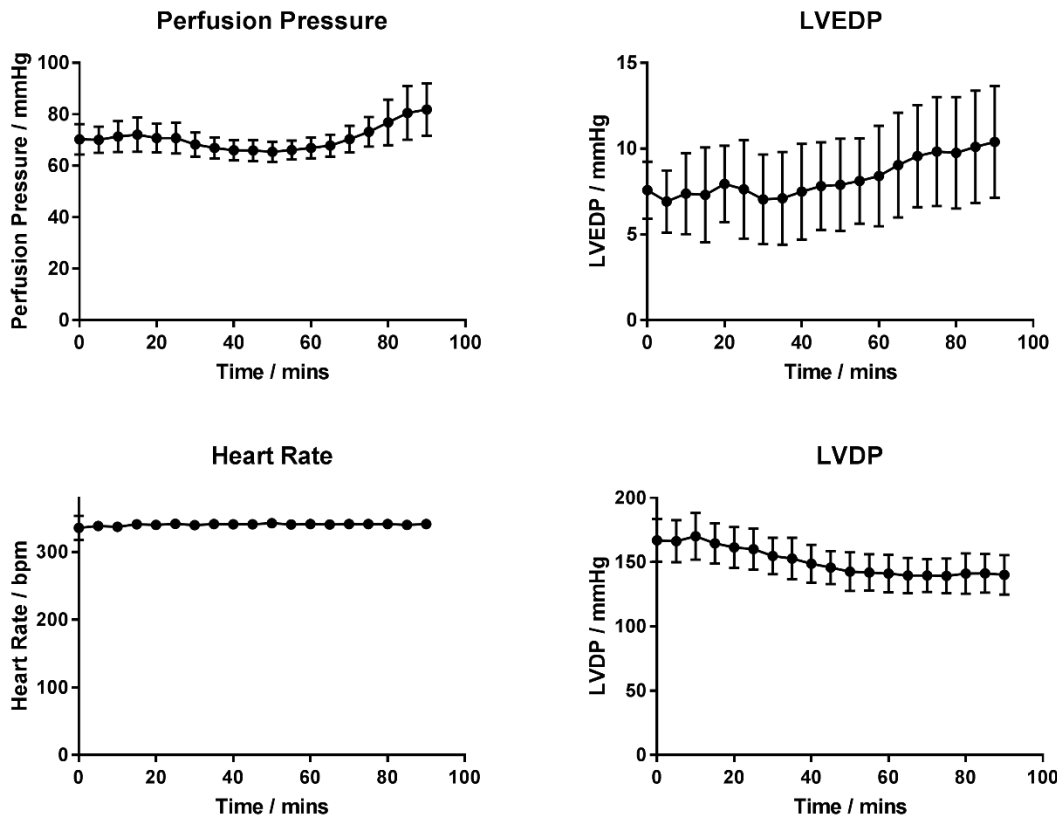


Figure S38: Stability study performed to generate exclusion criteria for the function of isolated perfused hearts. Clockwise from top left: perfusion pressure, left ventricular end diastolic pressure (LVEDP), left ventricular developed pressure (LVDP), heart rate. Perfusion pressure was measured by a pressure transducer connected to the arterial line, whilst LVEDP, LVDP and heart rate were calculated as a function of the left ventricular pressure measured by an isovolumetric balloon connected to a pressure transducer inserted into the left ventricle. Hearts were electrically paced at  $340 \text{ min}^{-1}$ . Data represents mean ( $n = 6$ )  $\pm$  SD.

## Effects of 600 nM CCCP Infusion on Haemodynamic Parameters

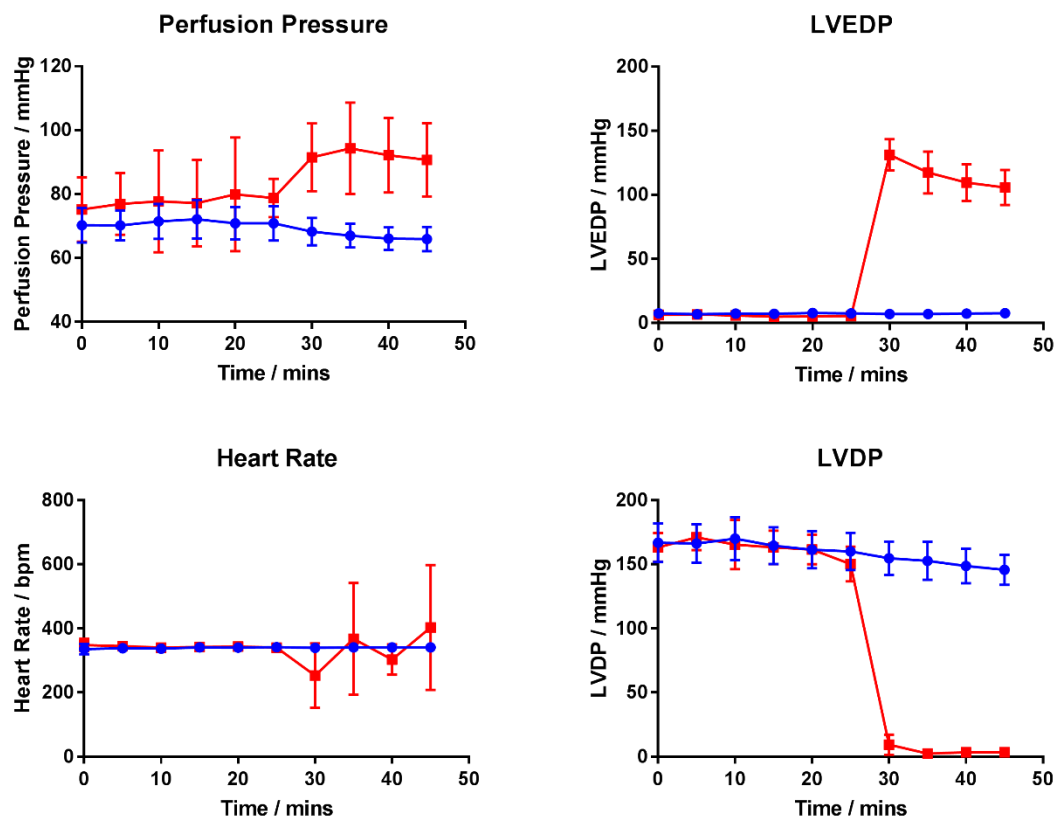


Figure S39: Haemodynamic parameters for control hearts undergoing normal function for 45 minutes ( $n = 6$ , blue) and hearts undergoing normal function for 25 minutes followed by infusion with 600 nM CCCP for 20 minutes ( $n = 4$ , red). Clockwise from top left: perfusion pressure, LVEDP, LVDP, heart rate. Data represents mean  $\pm$  SD.

### Triple $\gamma$ -Detector System Raw Data for MIBI Using the Two-Injection Protocol

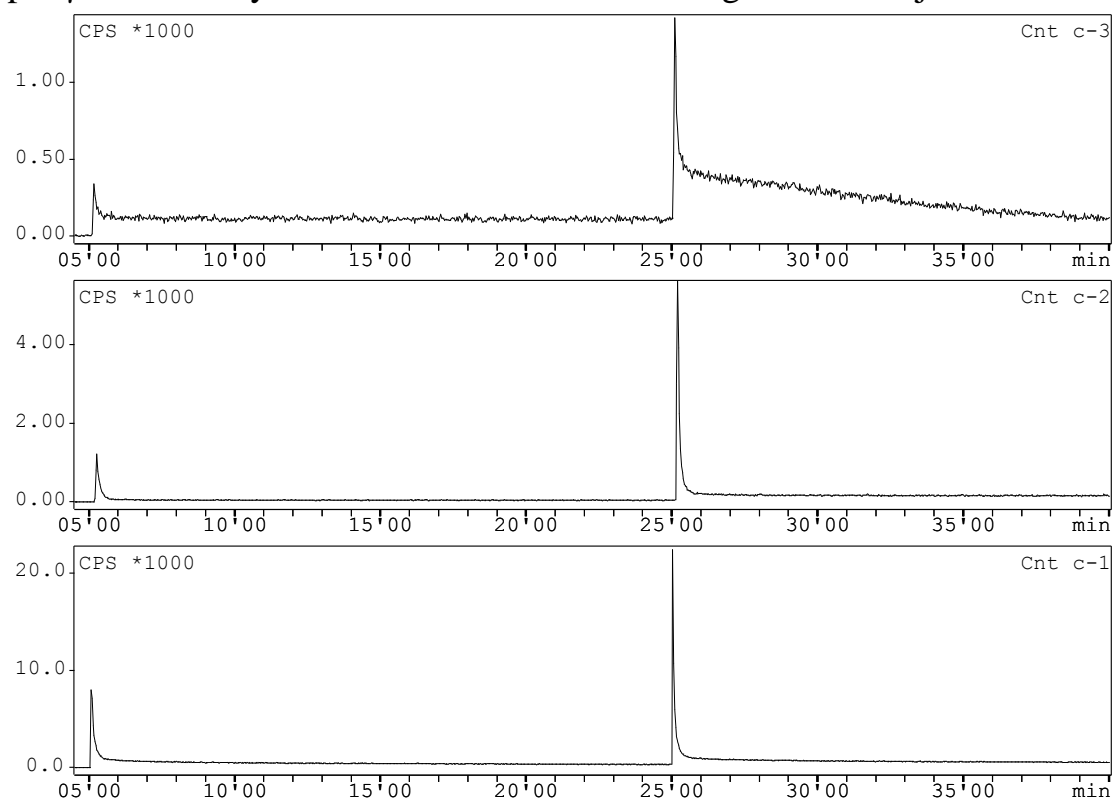


Figure S40: Experiment 1. N.B. The heart detector is Cnt c-3.

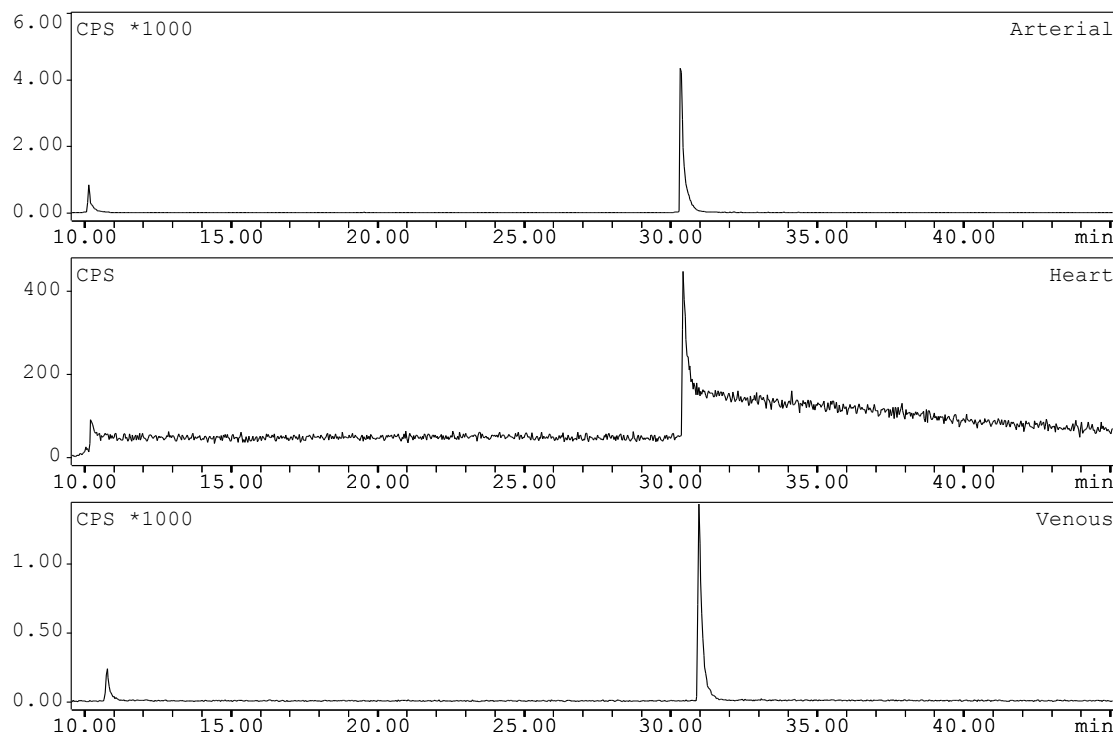


Figure S41: Experiment 2

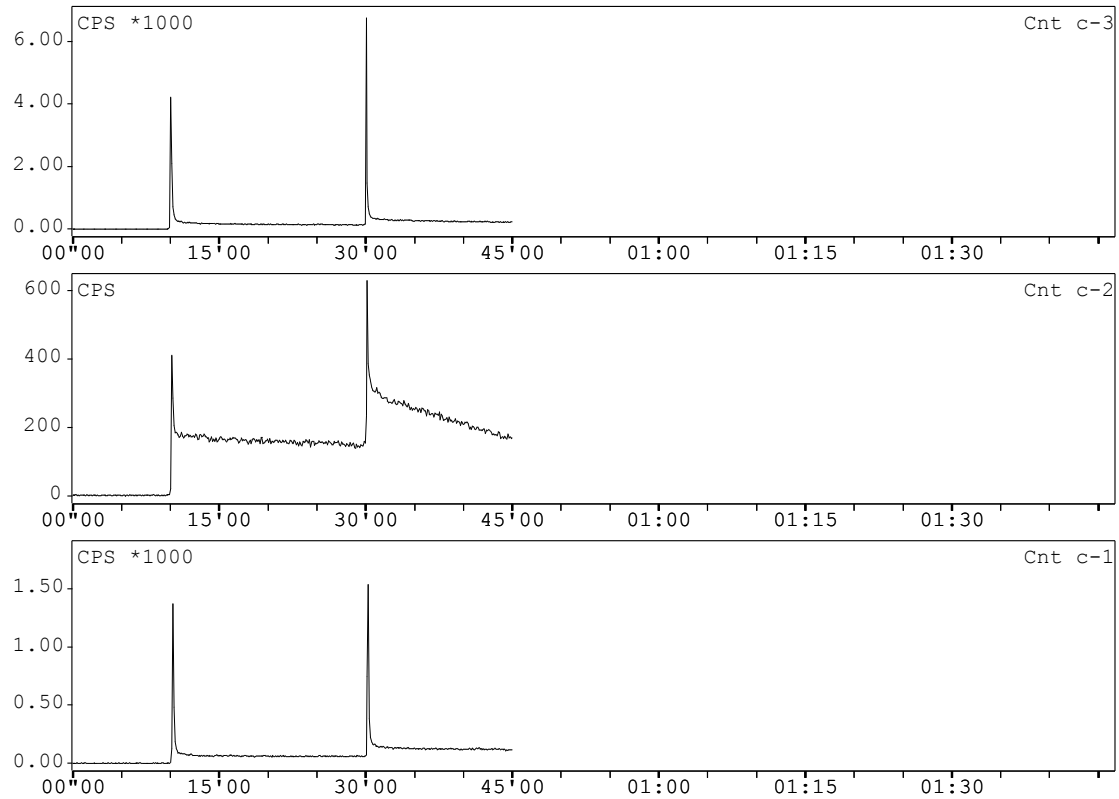


Figure S42: Experiment 3. For this and all following experiments, the arterial detector is Cnt c-3, the heart detector is Cnt c-2, and the venous washout is Cnt c-1.

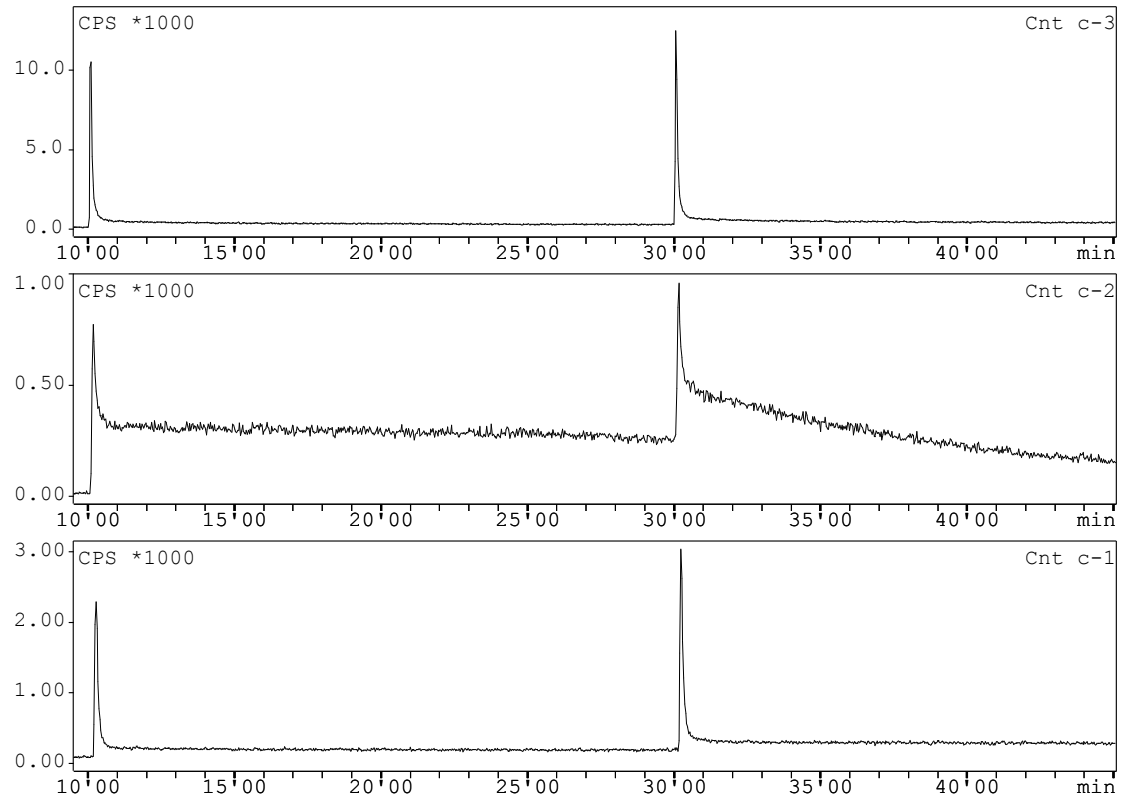


Figure S43: Experiment 4

Triple  $\gamma$ -Detector System Raw Data for  $[^{68}\text{Ga}]\text{Ga-DO3A-xy-TXP}$  Using the Two-Injection Protocol

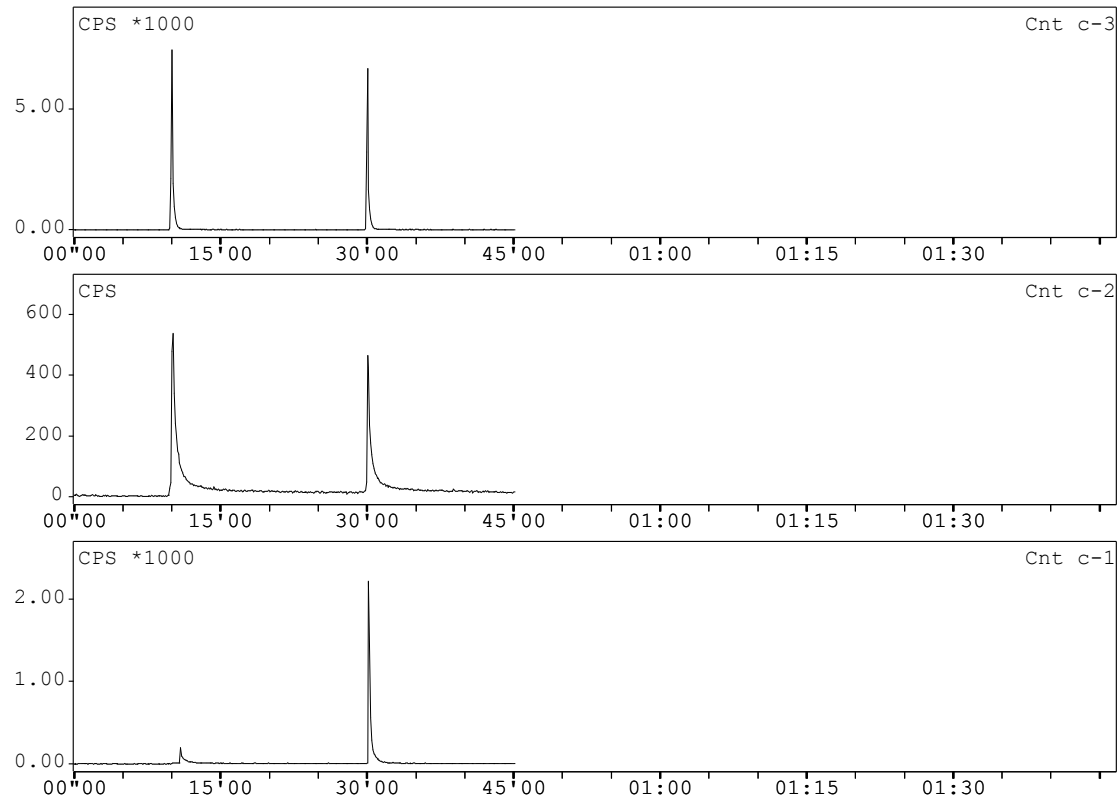


Figure S44: Experiment 1

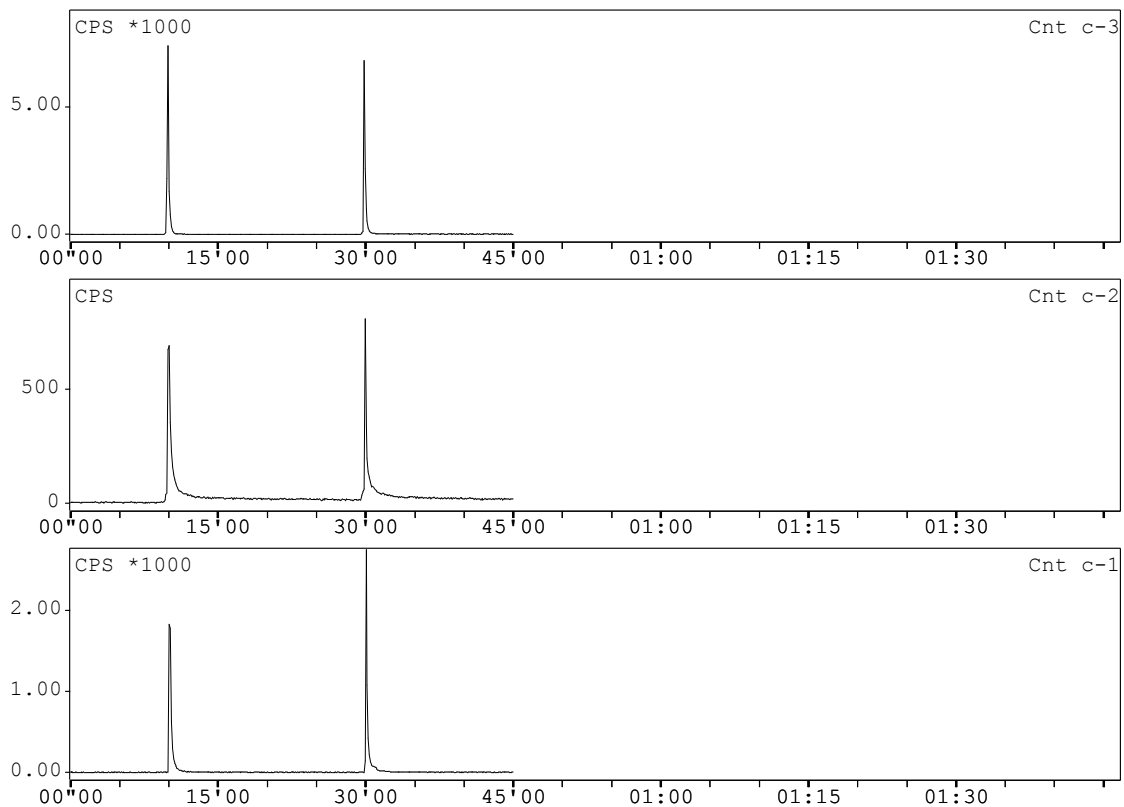


Figure S45: Experiment 2

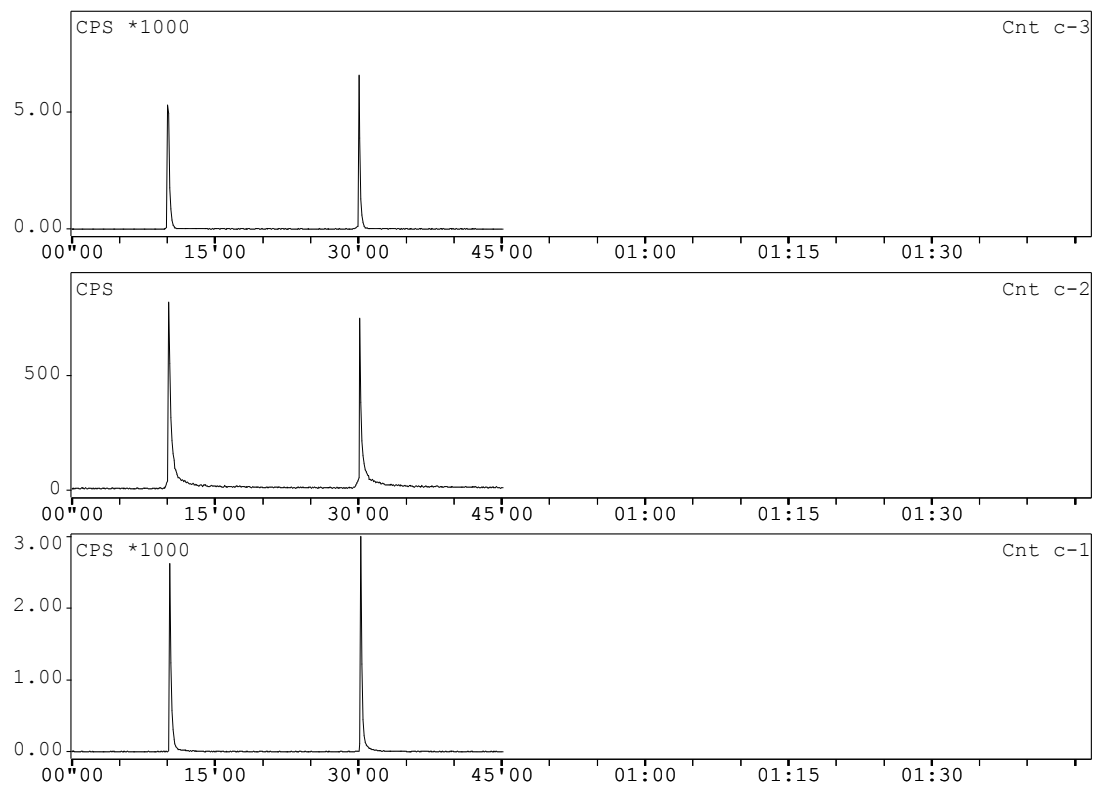


Figure S46: Experiment 3